



AGR-5/6/7 Irradiation As-Run Predictions Using PARFUME

September 2021

William F. Skerjanc



*INL is a U.S. Department of Energy National Laboratory
operated by Battelle Energy Alliance, LLC*

DISCLAIMER

This information was prepared as an account of work sponsored by an agency of the U.S. Government. Neither the U.S. Government nor any agency thereof, nor any of their employees, makes any warranty, expressed or implied, or assumes any legal liability or responsibility for the accuracy, completeness, or usefulness, of any information, apparatus, product, or process disclosed, or represents that its use would not infringe privately owned rights. References herein to any specific commercial product, process, or service by trade name, trade mark, manufacturer, or otherwise, does not necessarily constitute or imply its endorsement, recommendation, or favoring by the U.S. Government or any agency thereof. The views and opinions of authors expressed herein do not necessarily state or reflect those of the U.S. Government or any agency thereof.

AGR-5/6/7 Irradiation As-Run Predictions Using PARFUME

William F. Skerjanc

September 2021

**Idaho National Laboratory
Advanced Reactor Technologies
Idaho Falls, Idaho 83415**

<http://www.art.inl.gov>


**Prepared for the
U.S. Department of Energy
Office of Nuclear Energy
Under DOE Idaho Operations Office
Contract DE-AC07-05ID14517**

Page intentionally left blank

INL ART Program
AGR-5/6/7 Irradiation As-Run Predictions Using
PARFUME
INL/EXT-21-64576

September 2021


Technical Reviewer:



Jason D. Hales
Computational Mechanics and Materials Manager

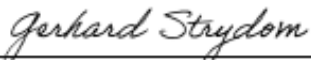
27 Sep 2021
Date

Approved by:



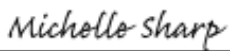
Paul A. Demkowicz
AGR Fuels Technical Director

9/29/2021
Date



Gerhard Strydom
INL ART Director

9/29/2021
Date



Michelle T. Sharp
INL Quality Assurance

9/30/2021
Date

ABSTRACT

The PARticle FUEl Model (PARFUME), a fuel performance modeling code used for high-temperature gas-cooled reactors, was used to model the Advanced Gas Reactor (AGR)-5/6/7 irradiation test using as-run physics and thermal data. The AGR-5/6/7 irradiation test consists of the combined fifth, sixth, and seventh planned irradiations of the AGR Fuel Development and Qualification Program. The AGR-5/6/7 test train was a multi-capsule, instrumented experiment that was designed for irradiation in the 133.4-mm diameter northeast flux trap position of the Advanced Test Reactor (ATR) at Idaho National Laboratory. Each capsule contained compacts filled with uranium oxycarbide tristructural isotropic (TRISO)-coated fuel particles. This report documents the calculations performed to predict the failure probability of TRISO fuel particles during the AGR-5/6/7 experiment. In addition, this report documents the calculated fission product release fraction from the fuel. The calculations include modeling of the AGR-5/6/7 irradiation that occurred from February 2018 to July 2020 over nine ATR cycles, including six normal cycles and three power axial locator mechanism cycles, for a total of approximately 376 effective full power days (EFPD).

The irradiation conditions and material properties of the AGR-5/6/7 test predicted zero fuel particle failures in capsules 1, 3, and 4. Fuel particle failures were predicted in two of the compacts in capsule 2 and one particle failure is predicted in each one of the compacts in capsule 5. All compacts that exhibited fuel particle failures predicted by PARFUME were caused by localized stress concentrations in the silicon carbide (SiC) layer caused by cracking in the inner pyrolytic (IPyC) layer.

In addition, shrinkage of the buffer and IPyC layer during irradiation resulted in formation of a buffer-IPyC gap. Compacts with a lower irradiation temperature and fluence experienced the smallest buffer-IPyC gap formation. Conversely, higher irradiated temperature compacts with a high fluence experienced the largest buffer-IPyC gap formation. Compact 3-6-3 experienced the largest buffer-IPyC gap formation of just under 21.7 μm .

The calculated release fraction of fission products silver (Ag), cesium (Cs), and strontium (Sr) varied depending on capsule location and irradiation temperature. The maximum release fraction of Ag occurred in capsule 3, reaching up to 59.5% for the TRISO fuel particles (compact 3-6-3). The release fractions of the other two fission products, Cs and Sr, were much smaller. A

maximum Cs release fraction of 1.1% occurred in compact 3-4-3 and 4.4% for Sr in compact 3-6-3.

Page intentionally left blank

CONTENTS

ABSTRACT.....	iv
ACRONYMS.....	x
1. INTRODUCTION.....	1
1.1 AGR Program	1
1.2 PARFUME.....	2
2. AGR-5/6/7 IRRADIATION EXPERIMENT	2
2.1 AGR-5/6/7 Irradiation Description	2
3. PARFUME MODELING.....	6
3.1 Boundary/Irradiation Conditions	6
3.2 Input Parameters	10
3.3 Multidimensional Stress.....	11
3.4 Material Properties	11
3.5 Physico-Chemical Behavior.....	12
3.6 Failure Mechanisms Considered.....	12
4. RESULTS	13
4.1 Fuel Particle Failure Probability	13
4.2 Buffer-IPyC Gap	16
4.3 Fission Product Release Fraction	18
5. CONCLUSION	20
6. REFERENCES.....	20
Appendix A Fuel Particle Failure Probability.....	22
Appendix B Fission Product Release.....	30

FIGURES

Figure 1. ATR core cross section displaying the NEFT position.....	3
Figure 2. Axial schematic of the AGR-5/6/7 test train.	3
Figure 3. Cross sections of the AGR 5/6/7 capsules showing the compact stacks.	4
Figure 4. Typical TRISO-coated fuel particle.	5
Figure 5. Fuel particle failure probability vs. temperature.....	14
Figure 6. Fuel particle failure probability vs. fluence.....	15
Figure 7. Fuel particle failure probability vs. burnup.	15
Figure 8. Buffer-IPyC gap width.	17
Figure 9. Particle temperature differential (kernel centerline to outer OPyC).....	17
Figure 10. Compact silver (Ag) release fraction versus temperature.....	18
Figure 11. Compact cesium (Cs) release fraction versus temperature.....	19
Figure 12. Compact strontium (Sr) release fraction versus temperature.....	19

TABLES

Table 1. AGR-5/6/7 capsules.	4
Table 2. Primary functions of particle fuel components.	5
Table 3. ATR AGR-5/6/7 irradiation schedule.....	6
Table 4. Compact accumulated fluence ($\times 10^{25}$ n/m ²) [$E_n > 0.18$ MeV].....	7
Table 5. Average compact burnup (% FIMA).	8
Table 6. Compact TAVA temperature at the end of irradiation (°C).....	9
Table 7. AGR-5/6/7 TRISO fuel particle geometry.....	10
Table 8. AGR-5/6/7 TRISO fuel particle attributes.	11
Table A1. AGR-5/6/7 capsule 5 fuel particle failure probability.....	23
Table A2. AGR-5/6/7 capsule 4 fuel particle failure probability.....	24
Table A3. AGR-5/6/7 capsule 3 fuel particle failure probability.....	25
Table A4. AGR-5/6/7 capsule 2 fuel particle failure probability.....	26
Table A5. AGR-5/6/7 capsule 1 fuel particle failure probability.....	27
Table B1. AGR-5/6/7 capsule 5 fission product release fraction.....	31
Table B2. AGR-5/6/7 capsule 4 fission product release fraction.....	32
Table B3. AGR-5/6/7 capsule 3 fission product release fraction.....	33
Table B4. AGR-5/6/7 capsule 2 fission product release fraction.....	34
Table B5. AGR-5/6/7 capsule 1 fission product release fraction.....	35

Page intentionally left blank

ACRONYMS

AGR	Advanced Gas Reactor
ATR	Advanced Test Reactor
CEGA	Combustion Engineering/General Atomics
DOE	Department of Energy
EFPD	effective full power day
FIMA	fissions per initial heavy metal atom
HTGR	High Temperature Gas Reactor
INL	Idaho National Laboratory
IPyC	inner pyrolytic carbon
NEFT	northeast flux trap
OPyC	outer pyrolytic carbon
PALM	power axial locator mechanism
PARFUME	PARticle FUEl ModEl
PIE	post-irradiation examination
SiC	silicon carbide
TAVA	time-average volume-average
TRISO	tristructural isotropic
UCO	uranium oxycarbide

Page intentionally left blank

AGR-5/6/7 Irradiation As-Run Predictions Using PARFUME

1. INTRODUCTION

Several fuel and material irradiation experiments were planned for the United States Department of Energy (DOE) Advanced Gas Reactor (AGR) Fuel Development and Qualification Program. These experiments support development and qualification of tristructural isotropic (TRISO)-coated particle fuel for use in high-temperature gas-cooled reactors. The goals of these experiments are to provide irradiation performance data to support fuel process development, qualify fuel for normal operating conditions, support development and validation of fuel performance and fission product transport models and codes, and provide irradiated fuel and materials for post-irradiation examination (PIE) and safety testing (Demkowicz 2021). AGR-5/6/7 combined the fifth, sixth, and seventh in this series of planned experiments to test TRISO-coated, low-enriched uranium oxycarbide (UCO) fuel.

This report documents the calculations performed to predict the failure probability of TRISO-coated fuel particles during the AGR-5/6/7 experiment using the PARTicle FUEL Model (PARFUME) computer code developed at Idaho National Laboratory (INL). In addition, this report documents the calculated source term from the fuel. The calculations include modeling of the AGR-5/6/7 irradiation that occurred from February 2018 to July 2020 in the Advanced Test Reactor (ATR) at INL over nine ATR cycles, including six normal cycles and three power axial locator mechanism (PALM) cycles (Pham 2021).

Section 2 of this report provides an overview of the AGR-5/6/7 irradiation experiment including the experiment description and irradiation conditions. Section 3 describes the PARFUME modeling and particle failure mechanisms considered. Results of the study are provided in Section 4 with the conclusions in Section 5. References are listed in Section 6.

1.1 AGR Program

The DOE AGR Fuel Development and Qualification program was established to qualify TRISO-coated fuel for use in High Temperature Gas Reactors (HTGRs). The primary goal of the program is to provide a baseline fuel qualification data set in support of the licensing and operation of a HTGR (Demkowicz 2021).

Seven fuel and material irradiation experiments were planned for the DOE AGR program. The overall objectives of these experiments are to (Demkowicz 2021):

- Develop fuel fabrication capabilities
- Perform fuels and materials irradiation
- Perform safety testing and PIE
- Improve fuel performance modeling
- Evaluate fission product transport and source term determination.

1.2 PARFUME

The modeling was performed using the computer code PARFUME. PARFUME (Miller 2018), a fuel performance analysis and modeling code, has been developed at INL for evaluating gas-reactor TRISO-coated particle fuel for prismatic, pebble bed, plate, and cylindrical type fuel geometries. PARFUME is an integrated mechanistic computer code that evaluates the thermal, mechanical, and physico-chemical behavior of TRISO-coated fuel particles and the probability for fuel failure given the particle-to-particle statistical variations in physical dimensions and material properties that arise during the fuel fabrication process. The objective of PARFUME is to physically describe both the mechanical and physico-chemical behavior of the fuel particle under irradiation and postulated accident conditions while capturing the statistical nature of the fuel. The PARFUME code has been developed to determine the failure probability of a population of fuel particles, accounting for most viable mechanisms that can lead to particle failure. In addition, PARFUME calculates fission product transport by determining the diffusion of fission products from the fuel through the particle coating layers and their subsequent release through the fuel graphitic matrix to the coolant boundary. The subsequent release of fission products is calculated at the compact level (release of fission products from the compact), but it can also be assessed at the particle level by adjusting the diffusivity in the fuel matrix to very high values. Furthermore, the diffusivity of each layer can be individually set to a high value (typically $10^{-6} \text{ m}^2/\text{s}$) to simulate a failed layer with no capability of fission product retention.

Calculations were performed with PARFUME Version 2.23 (as configured by the Revision Control System) compiled with Intel FORTRAN Compiler 11.1.073 on an SGI ICE X platform operating under SUSE Linux Enterprise Server 11. PARFUME was executed with its fast integration scheme to calculate the particle failure probabilities and with its Monte Carlo scheme to obtain the fractional releases of fission products. In addition, this study was conducted in accordance with quality standard NQA-1-2008/-1a-2009, “Quality Assurance Requirements for Nuclear Facility Applications” (ASME 2008).

2. AGR-5/6/7 IRRADIATION EXPERIMENT

As defined in the technical program plan for the AGR Fuel Development and Qualification Program (Demkowicz 2021), the objectives of the AGR-5/6/7 experiment are as follows:

1. Irradiate reference design fuel containing low-enriched UCO TRISO fuel particles to support fuel qualification.
2. Establish the operating margins for the fuel beyond normal operating conditions.
3. Provide irradiated fuel performance data and irradiate fuel samples for PIE and safety testing.

2.1 AGR-5/6/7 Irradiation Description

To achieve the test objectives outlined above, in accordance with requirements from the technical program plan, the AGR Fuel Development and Qualification Program (Demkowicz 2021), and the Irradiation Test Specification (Maki 2015), AGR-5/6/7 was irradiated in the northeast flux trap (NEFT) position of ATR. A cross-sectional view of the ATR core, which indicates the NEFT location, is displayed in Figure 1.

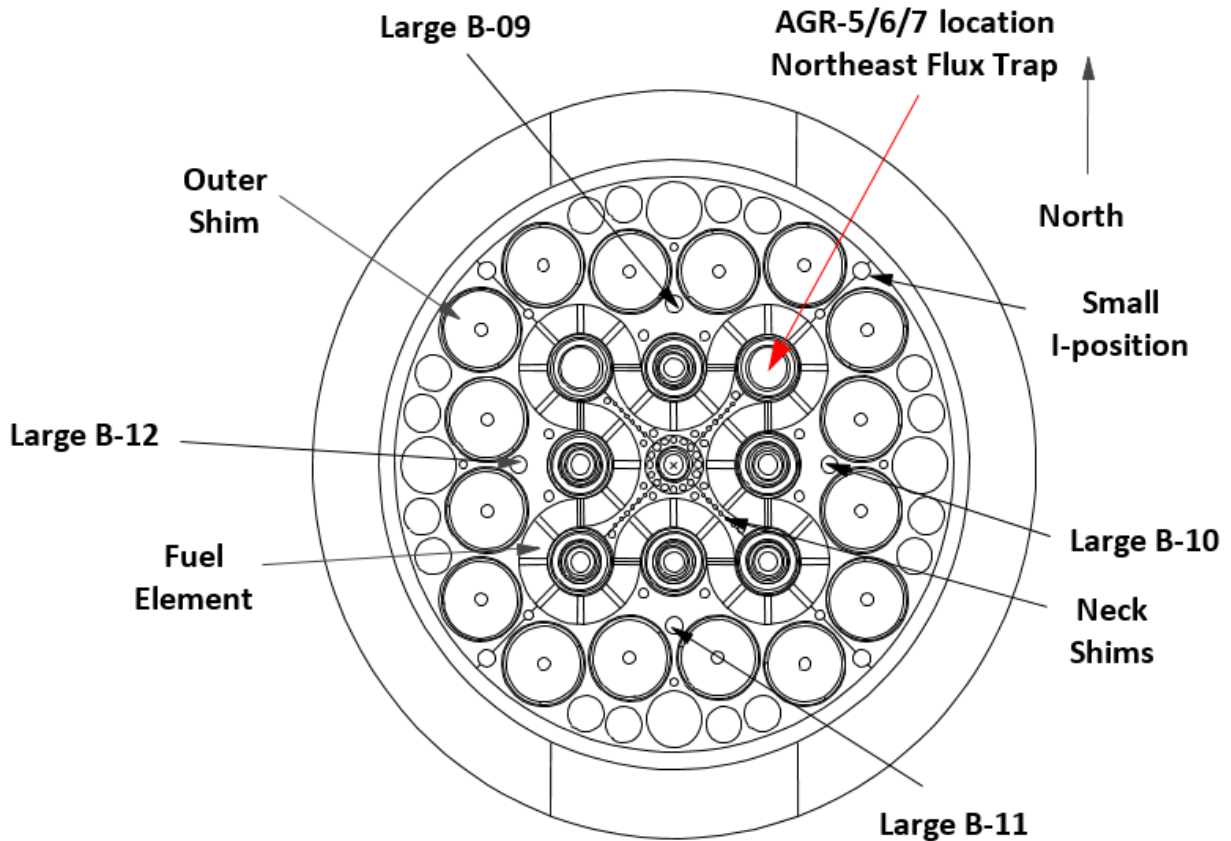


Figure 1. ATR core cross section displaying the NEFT position.

The AGR-5/6/7 test train was a multi-capsule, instrumented experiment that was designed for irradiation in the 133.4 mm diameter NEFT position of ATR. Figure 2 illustrates the axial schematic of the AGR-5/6/7 test train containing four AGR-5/6 capsules (capsules 1, 2, 4, and 5) and the AGR-7 capsule (capsule 3). Figure 3 illustrates the radial view of the capsules. A summary of the AGR-5/6/7 capsules is provided in Table 1 (Pham 2021).

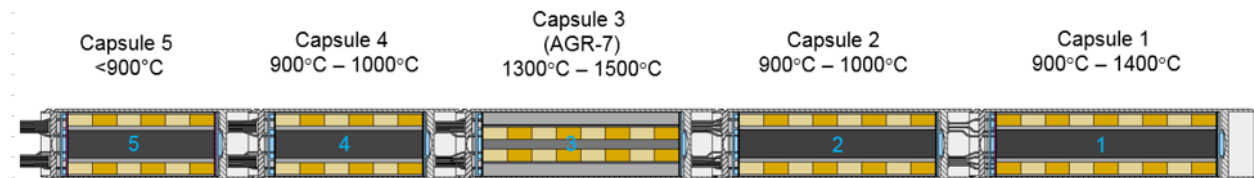


Figure 2. Axial schematic of the AGR-5/6/7 test train.

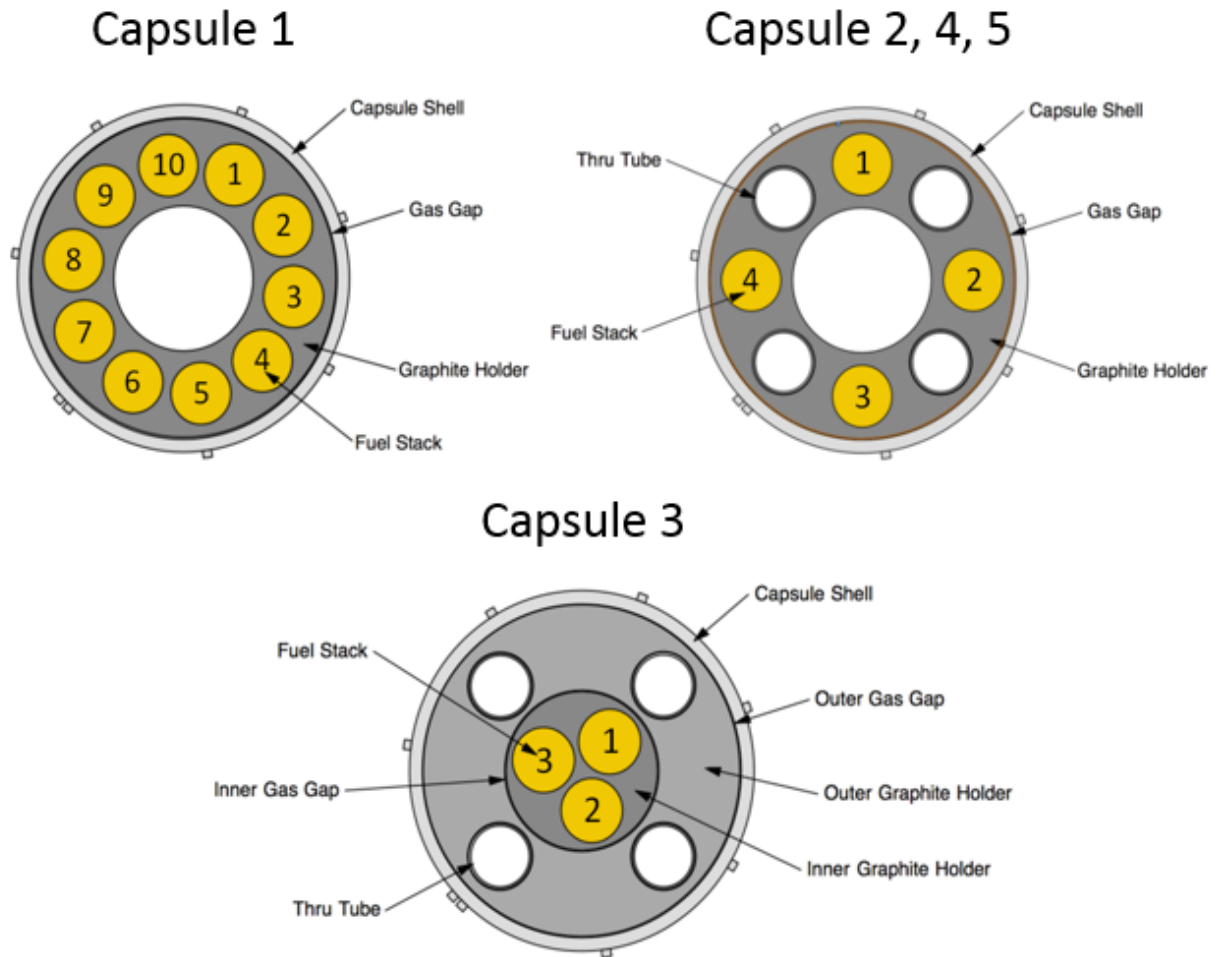


Figure 3. Cross sections of the AGR 5/6/7 capsules showing the compact stacks.

Table 1. AGR-5/6/7 capsules.

Capsule	Number of			Average Packing Fractions (%)	Approximate Number of Particles
	Levels	Stacks	Compacts		
5	6	4	24	38.4	3,393
4	6	4	24	24.9	2,197
3	8	3	24	25.5	2,265
2	8	4	32	25.5	2,265
1	9	10	90	38.4	3,434 / 3,393
AGR-5/6	--	--	170	--	515,700
AGR-7			24		54,360
Total			194		570,000

The AGR-5/6/7 experiment was irradiated for approximately 376 effective full power days (EFPDs). The minimum compact burnup value was determined to be 5.66% fissions per initial heavy metal atom (FIMA) in compact 1-1-2 and the maximum was 15.26% FIMA in compacts 2-7-4 and 2-8-4. Fast fluence ($E_n > 0.18$ MeV) values ranged between 1.62 (compact 1-1-2) and 5.55×10^{25} n/m² (compact 3-3-3) (Sterbentz 2020). Time-average volume-average (TAVA) fuel temperatures on a capsule basis at the end of irradiation ranged from 621°C in compact 5-6-2 to 1338°C in compacts 3-6-2 and 3-6-3 (Hawkes 2021). These irradiation conditions were obtained using two packing fractions of compacts in the test train. Compacts with a 38% nominal packing fraction were used in capsules 1 and 5, and compacts with a 25% nominal packing fraction were used in capsules 2, 3, and 4.

Fuel for AGR-5/6/7 contains reference design UCO TRISO-coated particles that are slightly less than 1 mm in diameter. Each particle has a central reference kernel that contains fuel material, a porous carbon buffer layer, an inner pyrolytic carbon (IPyC) layer, a silicon carbide (SiC) barrier coating, and an outer pyrolytic carbon (OPyC) layer as depicted in Figure 4. Each layer's function is described in Table 2. Kernels for AGR-5/6/7 consist of low-enriched UCO fuel.

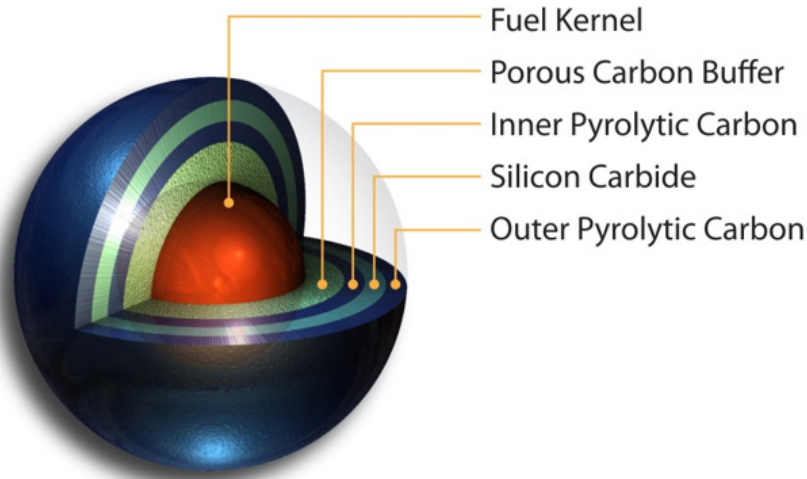


Figure 4. Typical TRISO-coated fuel particle.

Table 2. Primary functions of particle fuel components.

Component	Primary Function
Kernel	Contains fissile fuel.
Buffer	Provides void space for fission product gases and accommodates differential changes in dimensions between coating layers and kernel.
IPyC	Structural layer and fission gas barrier that protects the kernel during SiC deposition and the SiC layer from most fission products during irradiation.
SiC	Primary structural layer and primary fission product barrier.
OPyC	Structural layer that also permits embedding the particles in graphitic matrix material.

A complete description of the fuel kernels, particles, compacts, and physics and thermal analyses is presented in the AGR-5/6/7 test plan (Collin 2018).

The AGR-5/6/7 irradiation schedule is summarized in Table 3, presenting the cycle type and length to achieve the ~376 EFPD irradiation over the nine ATR power cycles (Sterbentz 2020).

Table 3. ATR AGR-5/6/7 irradiation schedule.

Cycle No.	ATR Cycle No.	ATR Cycle Type	Cycle Length (EFPD)
1	162B	Regular	38.83
2	163A	PALM	8.49
3	164A	Regular	55.61
4	164B	Regular	64.29
5	165A	PALM	13.82
6	166A	Regular	62.41
7	166B	Regular	61.20
8	167A	PALM	9.80
9	168A	Regular	61.22
Total			375.68

3. PARFUME MODELING

PARFUME was used to model the AGR-5/6/7 experiment to determine the probability of fuel particle failure and the release fractions of the fission products silver (Ag), cesium (Cs), and strontium (Sr) to determine the source term. The analysis considered conventional fuel particle failure (e.g., typical pressure vessel failure) and multidimensional failure mechanisms (e.g., IPyC cracking, asphericity, and debonding). The PARFUME modeling did not take into account any as-fabricated exposed kernels and the source terms were calculated assuming no fuel particle failures at time equal to zero. Key aspects of the PARFUME modeling of these AGR-5/6/7 conditions are described in the following subsections.

3.1 Boundary/Irradiation Conditions

PARFUME is designed to evaluate fuel performance based on user inputs for neutron fluence and burnup, with a corresponding set of thermal conditions. Results from neutronics analyses and measured values are possible sources for fluence and burnup inputs. For this analysis, compact-specific fluence and burnup results from neutronics (Sterbentz 2020) analysis and fuel temperature histories from thermal (Hawkes 2021) analysis performed to support the AGR-5/6/7 experiment campaign. It was determined that AGR-5/6/7 would have 194 compacts (Collin 2018) and the as-run PARFUME predictions were performed on a compact level basis using the daily TAVA temperatures. The fluence (Table 4), burnup (Table 5), and final TAVA temperatures (Table 6) for all the compacts used in this analysis are provided below.

Table 4. Compact accumulated fluence ($\times 10^{25}$ n/m²) [$E_n > 0.18$ MeV].

Capsule	Level	Stack									
		1	2	3	4	5	6	7	8	9	10
5	6	1.68	1.67	1.74	1.74						
	5	2.06	2.05	2.13	2.14						
	4	2.40	2.39	2.48	2.49						
	3	2.71	2.70	2.81	2.82						
	2	3.01	2.99	3.12	3.13						
	1	3.27	3.25	3.39	3.40						
4	6	4.01	4.00	4.18	4.20						
	5	4.24	4.23	4.42	4.44						
	4	4.42	4.40	4.61	4.62						
	3	4.57	4.55	4.77	4.79						
	2	4.70	4.68	4.90	4.93						
	1	4.80	4.78	5.01	5.03						
3	8	5.18	5.29	5.30							
	7	5.28	5.40	5.41							
	6	5.34	5.46	5.47							
	5	5.39	5.51	5.52							
	4	5.41	5.54	5.54							
	3	5.42	5.55	5.55							
	2	5.42	5.54	5.54							
	1	5.37	5.48	5.49							
2	8	5.21	5.20	5.44	5.44						
	7	5.18	5.17	5.42	5.42						
	6	5.13	5.12	5.36	5.36						
	5	5.05	5.04	5.28	5.29						
	4	4.96	4.95	5.18	5.19						
	3	4.85	4.85	5.07	5.07						
	2	4.72	4.72	4.94	4.94						
	1	4.56	4.56	4.77	4.77						
1	9	4.17	4.16	4.22	4.31	4.38	4.40	4.40	4.38	4.31	4.22
	8	4.00	4.00	4.06	4.14	4.21	4.23	4.23	4.21	4.14	4.06
	7	3.76	3.76	3.82	3.90	3.97	3.99	3.99	3.97	3.90	3.82
	6	3.49	3.49	3.54	3.62	3.68	3.70	3.70	3.68	3.62	3.55
	5	3.18	3.18	3.23	3.30	3.37	3.39	3.39	3.36	3.30	3.24
	4	2.85	2.84	2.89	2.96	3.02	3.04	3.04	3.02	2.96	2.89
	3	2.48	2.48	2.52	2.58	2.63	2.65	2.66	2.63	2.58	2.52
	2	2.07	2.07	2.11	2.16	2.21	2.23	2.23	2.20	2.16	2.11
	1	1.62	1.62	1.64	1.69	1.73	1.75	1.75	1.73	1.69	1.65

Table 5. Average compact burnup (% FIMA).

Capsule	Level	Stack									
		1	2	3	4	5	6	7	8	9	10
5	6	6.75	6.75	7.03	7.05						
	5	7.43	7.44	7.64	7.67						
	4	7.98	7.96	8.17	8.17						
	3	8.43	8.43	8.59	8.60						
	2	8.84	8.82	8.98	9.00						
	1	9.16	9.17	9.38	9.40						
4	6	12.37	12.36	12.62	12.65						
	5	12.84	12.83	13.11	13.15						
	4	13.24	13.22	13.52	13.56						
	3	13.55	13.53	13.83	13.87						
	2	13.72	13.70	14.03	14.07						
	1	13.78	13.73	14.06	14.10						
3	8	13.62	13.80	13.81							
	7	14.27	14.46	14.49							
	6	14.56	14.72	14.77							
	5	14.69	14.87	14.89							
	4	14.73	14.91	14.95							
	3	14.67	14.84	14.88							
	2	14.43	14.61	14.62							
	1	13.58	13.76	13.77							
2	8	14.93	14.93	15.25	15.26						
	7	14.92	14.92	15.25	15.26						
	6	14.89	14.88	15.21	15.21						
	5	14.78	14.78	15.09	15.09						
	4	14.60	14.61	14.91	14.92						
	3	14.38	14.36	14.67	14.69						
	2	14.03	14.02	14.33	14.33						
	1	13.52	13.52	13.82	13.82						
1	9	11.09	11.12	11.22	11.33	11.53	11.68	11.67	11.57	11.40	11.25
	8	10.43	10.44	10.49	10.59	10.75	10.89	10.91	10.76	10.62	10.50
	7	10.00	10.01	10.02	10.12	10.19	10.36	10.34	10.22	10.13	10.04
	6	9.61	9.61	9.63	9.68	9.79	9.88	9.86	9.78	9.70	9.64
	5	8.68	9.19	9.21	9.27	9.37	9.46	9.46	9.38	9.29	9.23
	4	8.11	8.63	8.74	8.80	8.95	9.05	9.03	8.95	8.82	8.74
	3	7.34	8.11	8.15	8.26	8.40	8.50	8.50	8.40	8.29	8.17
	2	7.34	7.35	7.42	7.56	7.71	7.84	7.85	7.73	7.58	7.42
	1	5.78	5.66	5.86	6.13	6.47	6.63	6.67	6.42	6.16	5.89

Table 6. Compact TAVA temperature at the end of irradiation (°C).

Capsule	Level	Stack									
		1	2	3	4	5	6	7	8	9	10
5	6	622	621	630	631						
	5	747	747	757	758						
	4	791	791	803	803						
	3	785	784	796	796						
	2	774	774	786	785						
	1	696	695	706	706						
4	6	765	763	773	774						
	5	865	864	876	877						
	4	888	888	901	902						
	3	875	875	889	888						
	2	850	849	863	863						
	1	758	757	769	769						
3	8	1192	1193	1193							
	7	1318	1319	1320							
	6	1336	1338	1338							
	5	1332	1334	1334							
	4	1335	1336	1336							
	3	1329	1330	1330							
	2	1293	1295	1295							
	1	1167	1169	1169							
2	8	743	742	753	753						
	7	808	808	820	819						
	6	821	822	835	834						
	5	835	836	850	848						
	4	858	859	874	871						
	3	857	857	872	870						
	2	828	828	842	840						
	1	736	736	748	746						
1	9	934	936	939	944	949	952	952	950	944	937
	8	1075	1077	1081	1087	1093	1097	1097	1094	1088	1079
	7	1073	1072	1076	1082	1091	1096	1097	1094	1088	1079
	6	1048	1047	1050	1056	1066	1072	1073	1071	1064	1055
	5	1036	1035	1038	1044	1053	1061	1064	1060	1053	1043
	4	1011	1009	1012	1020	1029	1037	1040	1036	1028	1018
	3	951	950	954	961	971	979	980	976	968	958
	2	869	868	872	880	888	896	897	892	885	876
	1	750	749	752	759	767	772	773	768	761	754

PARFUME has considerable flexibility relative to the application of thermal conditions affecting fuel particles. A user may define the thermal conditions for the outer surfaces of the fuel-bearing materials (e.g., the outer surface of a pebble in the case of a pebble bed reactor or the coolant channel surface of a unit cell containing fuel compacts in the case of a prismatic reactor) or the user may define fuel-bearing material temperatures directly. Options for the outer surfaces of the fuel-bearing materials include defining either a time-dependent set of temperatures or a time-dependent set of heat transfer coefficients, with a corresponding time-dependent set of sink temperatures. Fuel-bearing material temperatures can be defined directly as time-dependent values that are applicable to the entire material or the user may divide the material into regions and supply time-dependent temperatures for each region. The direct specification of fuel-bearing material temperatures was applied here at the outer surface of the OPyC layer using the predicted irradiation temperatures (Hawkes 2021).

The modeling of fission product release was made on a compact basis; therefore, its results could be used as a source term to support the PIE effort on fission product transport. Prior PARFUME calculations were performed using the anticipated irradiation conditions (Skerjanc 2017) whereas this analysis was completed post-irradiation using the actual daily temperatures to produce a more accurate source term. The actual predicted failure fractions of the IPyC, silicon carbide (SiC), and OPyC were used, and they have a direct impact on the diffusion of fission products through the particle. When one of these layers fail, the diffusivity is reduced essentially opening that layer for free migration through that layer. Once the AGR-5/6/7 PIE has been completed identifying the number of actual fuel particle failures, PARFUME or an equivalent fuel performance code will be used for further analysis, in a manner similar to that performed for AGR-2 (Skerjanc 2020).

3.2 Input Parameters

PARFUME input parameters for modeling the AGR-5/6/7 irradiation experiment were taken from the final as-run report (Pham 2021) and the fuel product specification report (Marshall 2017). The fuel particle geometry and material properties are listed in Table 7 and Table 8, respectively. Statistical variations are considered relative to the fuel particle geometry only (e.g., kernel diameter, buffer, pyrolytic carbon, and SiC thicknesses). PARFUME also has the capability to address statistical variations in creep, bond strength, PyC densities, and PyC Bacon Anisotropy Factors (BAF). A further description of the treatment of statistical variations used in PARFUME can be found in the *PARFUME Theory and Model Basis Report* (Miller 2018).

Table 7. AGR-5/6/7 TRISO fuel particle geometry.

Attribute	Units	Mean Value	Standard Deviation
Kernel Diameter	μm	425.78	10.42
Buffer Thickness	μm	100.37	5.55
IPyC Thickness	μm	39.24	1.26
SiC Thickness	μm	36.15	0.65
OPyC Thickness	μm	35.03	1.99
Particle Sphericity	μm	1.04	0.02

Table 8. AGR-5/6/7 TRISO fuel particle attributes.

Attribute	Units	Mean Value	Standard Deviation
Kernel Density	Mg/m ³	11.048	--
Buffer Density	Mg/m ³	1.031	--
IPyC Density	Mg/m ³	1.897	0.099
OPyC Density	Mg/m ³	1.897	0.004
IPyC Bacon anisotropy factor		1.031	0.002
OPyC Bacon anisotropy factor		1.021	0.001
PyC Poisson's Ratio in Creep		0.5	--
U-235 Enrichment	weight %	15.477	--
Oxygen-to-Uranium	atom ratio	1.441	--
Carbon-to-Uranium	atom ratio	0.370	--

3.3 Multidimensional Stress

In addition to the one-dimensional behavior of a symmetrical spherical fuel particle, PARFUME considers multidimensional behavior, including aspherical geometry, cracking of the IPyC layer, and partial debonding of the IPyC from the SiC. To model these effects, PARFUME uses the results of detailed finite element analyses for cracked, debonded, and/or aspherical particles in conjunction with results from the PARFUME, closed form, one-dimensional solution to make a statistical approximation of the stress levels in any particle (Miller et al. 2003; Miller et al. 2004). Abaqus Version 6.9-2 (Abaqus 2009) was used to perform the finite element stress analyses to capture the multidimensional effects of asphericity and IPyC cracking. It has been previously determined that variations in parameters that greatly impact the multidimensional results include the IPyC, SiC, and OPyC thicknesses for both IPyC cracking and asphericity (Skerjanc 2016).

The degree to which the fuel particle is aspherical also impacts the probability of SiC failure due to pressure. The measured asphericity for AGR-5/6/7 was reported to be 1.053 at the SiC layer (Pham 2021). This corresponds to an aspect ratio of approximately 1.04 at the OPyC layer. The degree of asphericity used PARFUME requires the measurement made at the OPyC layer therefore the Abaqus calculations were made using an aspect ratio of 1.04 that corresponds to the sphericity at the OPyC level.

The PARFUME calculations for IPyC/SiC debonding was not performed in this analysis. Current fuel manufacturing practices, as demonstrated by previous AGR irradiation experiments, have greatly improved the IPyC/SiC bond strength resulting in zero fuel particle failures due to debonding during irradiation.

3.4 Material Properties

Material properties used in PARFUME are discussed in detail in the PARFUME Theory and Model Basis Report (Miller 2018). The elastic moduli and swelling strains for the IPyC and OPyC are treated as functions of fluence. The effective range for these properties extends to a fluence of 3.96×10^{25} n/m². However, an approximation was necessary to enable PARFUME modeling of some capsules in the AGR-5/6/7 test where the end-of-life fluence reaches as much as 5.55×10^{25} n/m². The approximation

consists of treating the elastic moduli and swelling strain rates as constants in PARFUME beyond a fluence level of $3.96 \times 10^{25} \text{ n/m}^2$ ($E_n > 0.18 \text{ MeV}$).

The historical creep coefficient for the pyrocarbon layers (Combustion Engineering/General Atomics (CEGA)1993) was found to be significantly lower than what has been used in other fuel performance models. It has also been found that PARFUME gives favorable comparisons with results of the New Production - Modular High Temperature Gas Reactor experiments if the historical creep coefficient is approximately doubled (Miller 2003). Therefore, the creep coefficient used in predictions for the AGR-5/6/7 test was set equal to twice the CEGA value.

There is significant uncertainty in how well certain physical properties of the coating layers are known. The accuracy of the failure probability predictions from any fuel performance code relies on the accuracy of these properties.

3.5 Physico-Chemical Behavior

A complete description of the treatment of the physico-chemical behavior can be found in the PARFUME Theory and Model Basis Report (Miller 2018).

The internal gas pressure is calculated in PARFUME as a function of time according to the Redlich-Kwong equation of state. Parameters utilized in this equation are derived from the critical temperature and pressure of each gas species occupying the void volume within the particle. PARFUME considers generation of carbon monoxide and release of the noble gas fission products (i.e., xenon and krypton) in this pressure calculation.

Carbon monoxide production can be calculated in PARFUME using an algorithm derived from thermochemical-free energy-minimization calculations performed by the HSC computer code. However, for this analysis, carbon monoxide production was not calculated since it is minimal in UCO fuel. PARFUME calculates fission-product gas release caused by both recoil and diffusion. Direct fission recoil from the kernel to the buffer is accounted for by geometrical considerations and fission fragment ranges derived from compiled experimental data. Diffusive release is calculated according to the Booth Equivalent Sphere Diffusion model, which utilizes an effective diffusion coefficient formulated by Turnbull. This effective diffusion coefficient accounts for intrinsic, thermal, and irradiation-enhanced diffusion.

3.6 Failure Mechanisms Considered

Five potential failure mechanisms are currently considered in PARFUME. The first is a pressure vessel failure caused by buildup of gases (e.g., fission, carbon monoxide). Stresses for this failure mechanism are determined using the one-dimensional solution in PARFUME for a three-layer (IPyC-SiC-OPyC) particle. Because of asphericity in the particle shape, these stresses are modified based on the results of the finite element analysis of aspherical particles. The particles' internal pressures in the AGR-5/6/7 irradiation test were not sufficient enough to cause any fuel particle failures as calculated by PARFUME.

The second mechanism considered is failure of the SiC layer caused by partial debonding of the IPyC from the SiC. Debonding, if it occurs, results from the IPyC shrinking inward away from the SiC during irradiation. PARFUME first determines whether debonding between the layers occurs by comparing the radial stress between layers with the bond strength between layers. If debonding is determined to occur, then the code estimates the stress in the SiC layer and accounts for the multidimensional effects using a previously documented methodology (Miller 2004). Because AGR-5/6/7 particle fabrication was based on German processes, the bond strength was set at a value that is considered to be representative for German particles (i.e., 100 MPa). At this bond strength, IPyC/SiC debonding was not predicted; therefore, debonding did not contribute to particle failures in the AGR-5/6/7 test.

The third failure mechanism considered in PARFUME is migration of the fuel kernel into the SiC layer under the influence of a temperature gradient (or the amoeba effect). This effect is driven by the production of carbon monoxide and is only prominent with uranium dioxide (UO₂) kernels and is limited with UCO kernels. Therefore, the amoeba effect made no contribution to particle failures in these analyses.

The fourth failure mechanism currently considered in PARFUME is failure of the SiC layer caused by irradiation-induced shrinkage and the associated cracking of the IPyC layer. The presence of a crack in the IPyC layer creates a stress concentration in the SiC layer. To treat the multidimensional effects of this stress concentration, PARFUME estimates stresses in the SiC layer that result from the presence of a crack based on a previously documented methodology. In evaluating failures caused by IPyC cracking, PARFUME first determines whether the IPyC layer cracks using the Weibull statistical theory. If the IPyC layer is predicted to crack, the particle is evaluated for failure of the SiC layer due to the presence of the crack. Some fuel particle failures in AGR-5/6/7 test calculations were found to be caused by this mechanism.

Chemical attack of the SiC layer by palladium (Pd) represents the fifth and final potential failure mechanism. This is modeled in PARFUME by calculating the penetration of palladium in the SiC layer. The penetration rate is calculated by an Arrhenius function fitted to all available in-reactor data for Pd penetration in SiC (Miller 2018). Failure occurs when penetration through the thickness of the SiC is complete, leading to the direct release of fission products. There were no fuel particle failures calculated by PARFUME in the AGR-5/6/7 irradiation by this mechanism.

PARFUME uses the Weibull statistical theory to determine whether particles fail using a mean strength for the SiC layer based on a stress distribution corresponding to the failure mechanism under consideration. The failure modes are implemented such that a particle fails only in the mode of failure that would occur first for that particle. The code retains the time at which the failures occur, allowing for construction of a time evolution of the failure probability for a batch of fuel particles. Weibull parameters that are used to evaluate failures of the SiC layer and cracking of the IPyC layer are discussed in the CEGA report (CEGA 1993). Failure of the SiC layer in PARFUME is assumed to lead to full TRISO failure.

4. RESULTS

Results from the AGR-5/6/7 as-run test predictions were obtained using PARFUME and are based on the inputs and modeling parameters discussed previously. These results include fuel particle failure probability, buffer-IPyC gap formation, and fission product release fractions. The results of particle failure probability were obtained using the fast (i.e., 2-loop) integration solver implemented in PARFUME as opposed to the full-loop integration or Monte Carlo method; this is due to the significant reduction in run times. It has been previously demonstrated that using the fast integration method does not adversely impact the accuracy of the results (Miller 2007). The fission product release calculations were run using the Monte Carlo scheme of PARFUME and the number of histories in these calculations were chosen to obtain the failure probabilities calculated by the integration scheme so that fission product release can take potential failures of the coating layers into account.

4.1 Fuel Particle Failure Probability

It is assumed that a fuel particle has failed when the SiC layer has become compromised and cracked, which leads to its inability to retain fission products. The primary mechanisms leading to SiC cracking and subsequent fuel particle failure in the AGR-5/6/7 analyses are due to IPyC cracking and pressure. It was determined that no fuel particle failure was predicted due to the amoeba effect or IPyC/SiC debonding. Complete results for the fuel particle failure probability analyses for the AGR-5/6/7 test are summarized in Appendix A and illustrated for all compacts in Figure 5 through Figure 7. Multiplying the number of particles per compact listed in Table 1 and rounding to the nearest integer, zero fuel particle

failures per compact analyzed were predicted in capsules 1, 2, 3, and 4 except for compacts 2-1-1 and 2-1-2 which each had one predicted fuel particle failure. PARFUME predicts one particle failure per compact analyzed in capsule 5. These SiC failures are due to the lower temperature causing less creep to counteract the shrinkage and causing the probability of IPyC cracking to increase. In general, fuel particle failures in capsule 5 can be attributed to IPyC cracking. Compact 3-6-3, at the maximum temperature, experienced a Pd penetration into the SiC layer of 16.9 μm , which is less than the actual SiC layer thickness (36.15 μm). The SiC layer is considered failed at 100% penetration but it is not linked to any failure probability calculations in PARFUME.

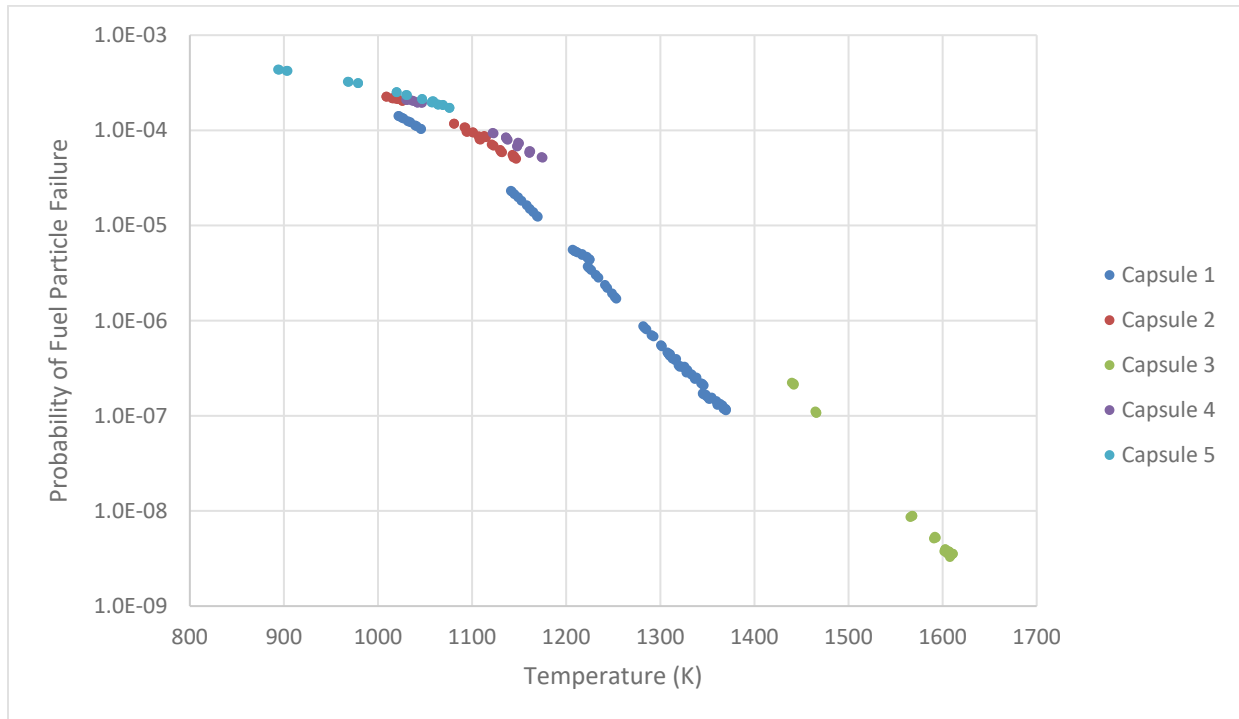


Figure 5. Fuel particle failure probability vs. temperature.

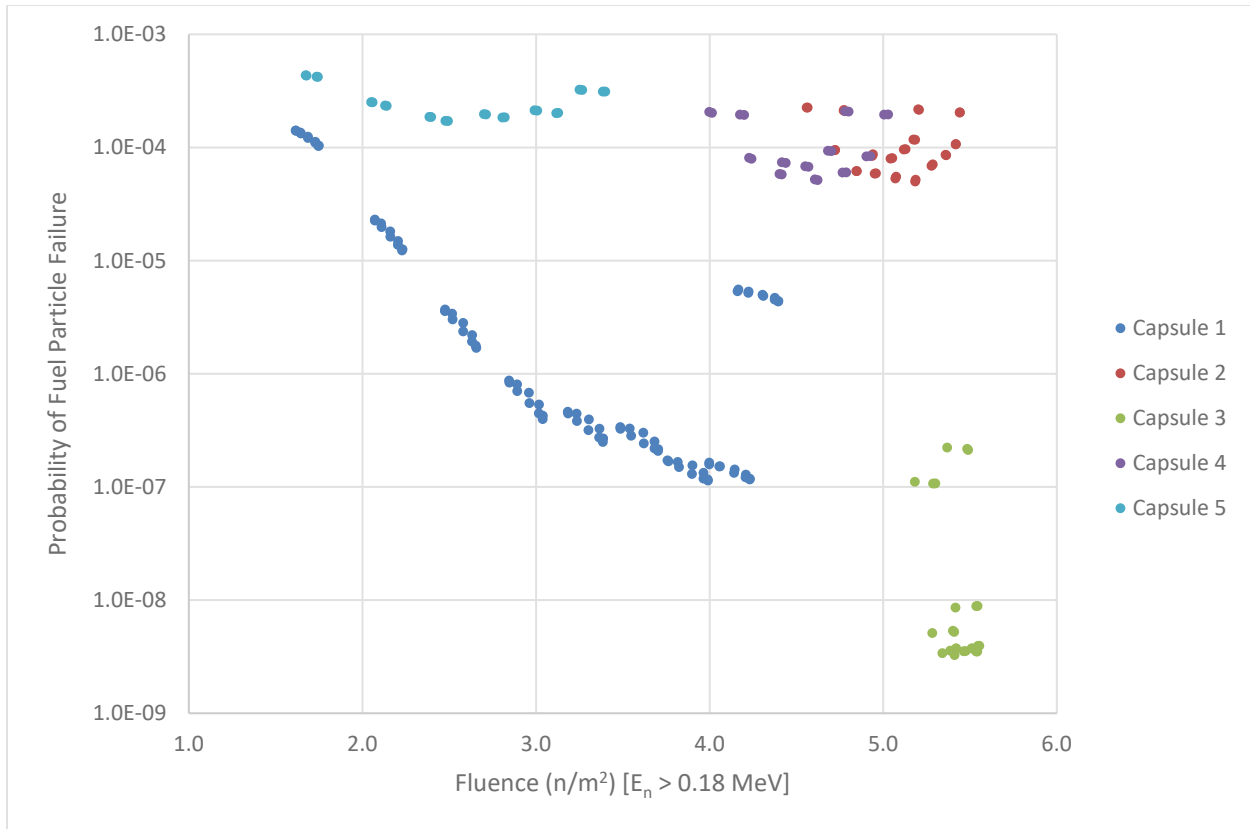


Figure 6. Fuel particle failure probability vs. fluence.

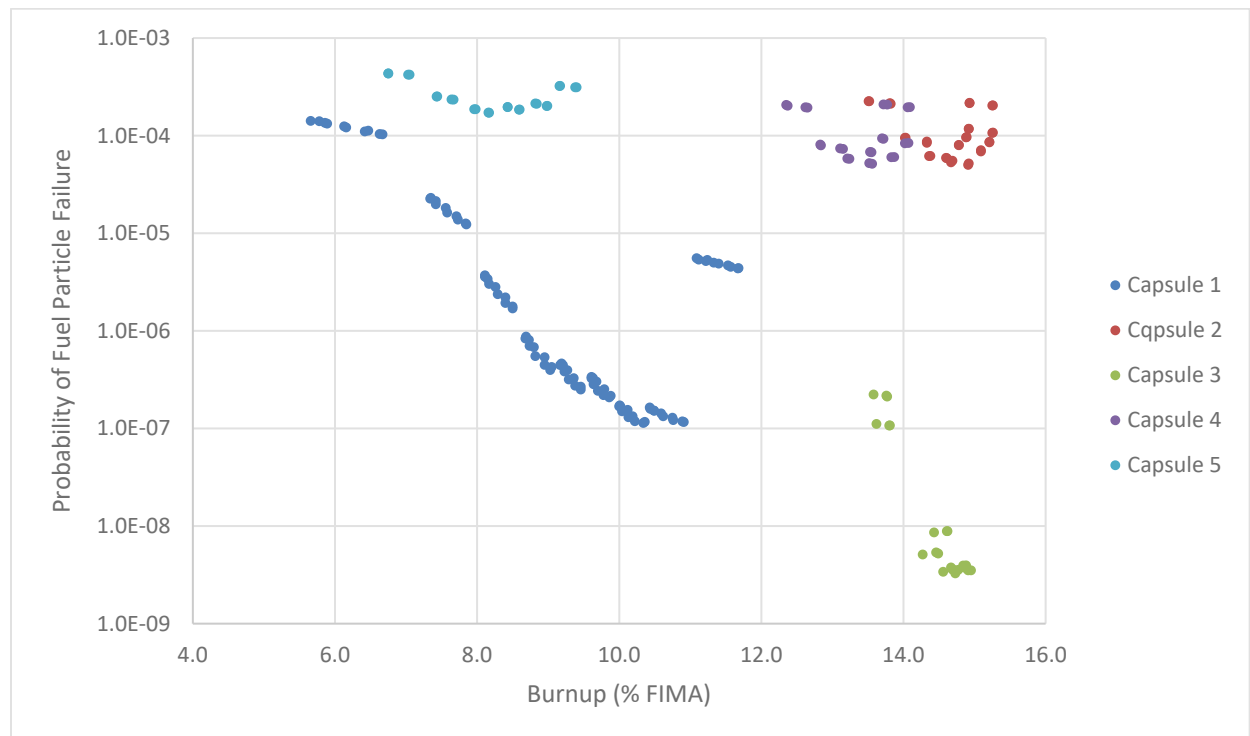


Figure 7. Fuel particle failure probability vs. burnup.

4.2 Buffer-IPyC Gap

Irradiation can lead to development of a gap between the buffer and IPyC layer. The gap can develop as a result of the combined effects of kernel swelling, shrinkage and creep in the buffer and IPyC layers, the effects of particle internal pressure, and the kernel/buffer contact pressure. However, differences in density between the buffer and the IPyC layer is a primary factor in the process. The buffer, which is much more porous than the dense IPyC layer, shrinks more during irradiation. The growth rate for the gap size slows as the buffer becomes denser during irradiation. PARFUME models the gap formation in 1-D geometry assuming the kernel/buffer remain concentrically centered inside the IPyC layer. The size of these gaps for the minimum and maximum compact temperatures for nominal particles is shown in Figure 8, assuming the outer surfaces of the OPyC layer in those particles is equal to compact-specific volume-averaged temperatures. Inspection of these figures indicates that the gap width is closely correlated with fluence, which is correlated with the axial position of the capsules in the ATR core. Because the axial neutron flux in ATR exhibits a cosine-like profile, gap widths tend to be smallest in compacts exposed to relatively low-fluence levels and largest in the compacts exposed to relatively high-fluence levels.

The buffer-IPyC gap can be a significant fraction of the thermal resistance in a fuel particle. Consequently, if other conditions are equal, temperature differentials (e.g., from the kernel centerline to the outer surface of the OPyC) are higher across particles with larger gaps. This trend is apparent in Figure 9 where temperature differentials are shown assuming the outer surfaces of particles follow volume-averaged temperatures. In this figure, temperature differentials are higher in center capsules' particles than in capsule 1 and 5 particles, which would be expected given the capsule-to-capsule differences in the buffer-IPyC gaps along with the higher temperatures in the center of the test train. In addition, the temperature differential is higher in compact 5-6-2 when compared to compact 1-1-2 even though compact 5-6-2 has a lower TAVA temperature. Both of these compacts have approximately the same end-of-irradiation fluence ($\sim 1.6 \times 10^{25}$ n/m²) but compact 5-6-2 had higher power level as demonstrated by an end-of-irradiation of 6.75% FIMA versus 5.66% FIMA for compact 1-1-2. The irradiation-induced dimensional changes are impacted by both the fluence and burnup history of the particle which then influences the size of the gap.

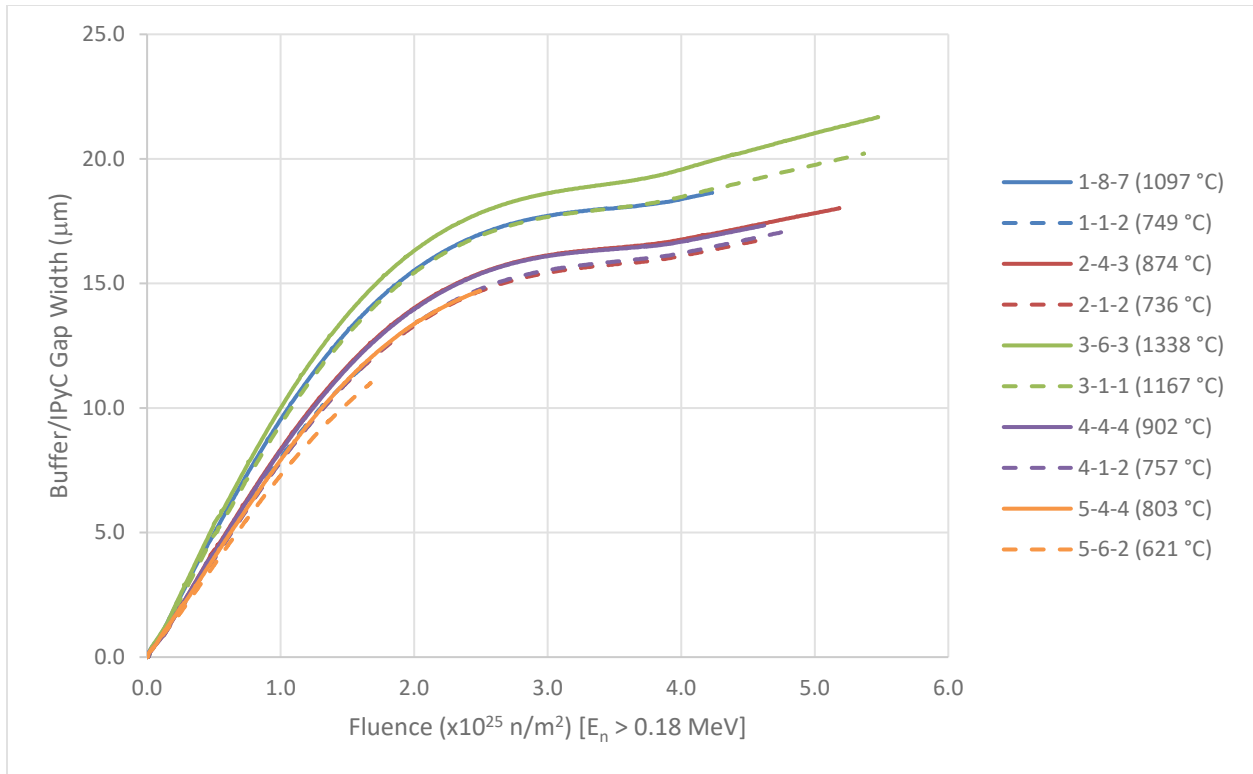


Figure 8. Buffer-IPyC gap width.

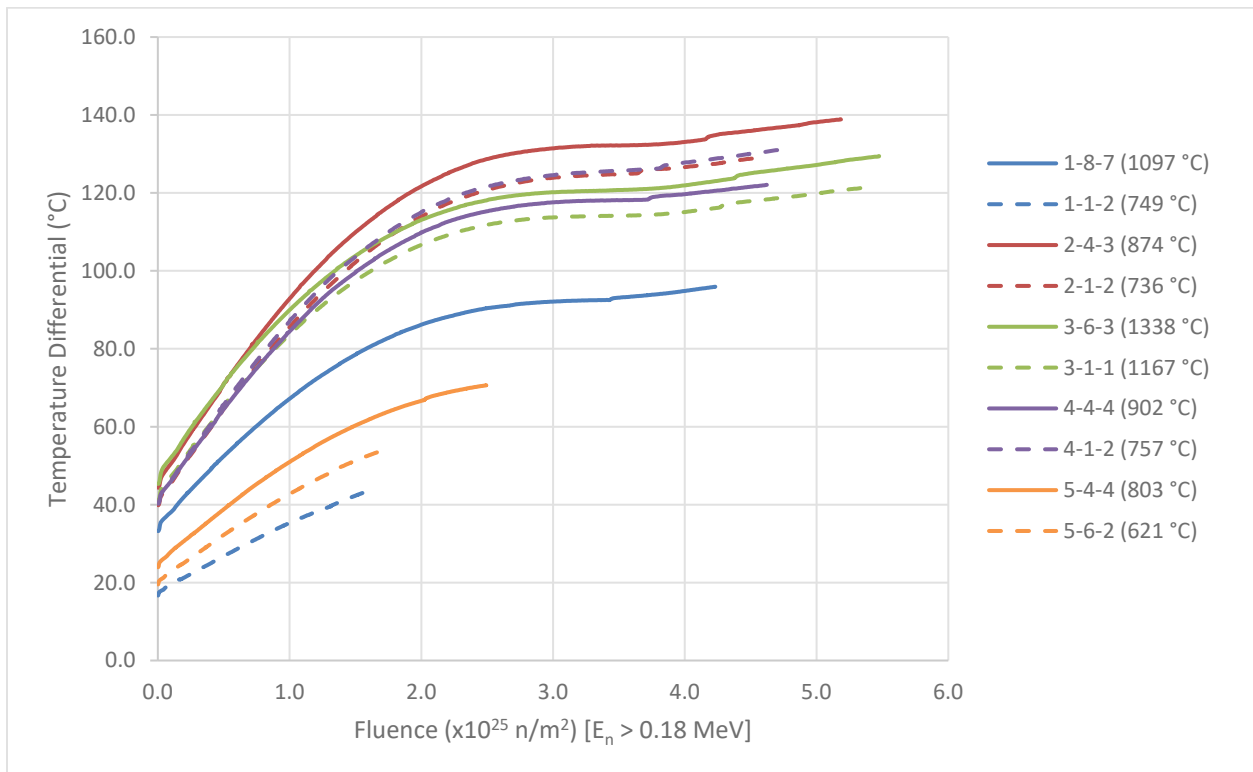


Figure 9. Particle temperature differential (kernel centerline to outer OPyC).

4.3 Fission Product Release Fraction

The release fraction—the ratio of the number of atoms released to the number of atoms generated—from the TRISO fuel particles was also analyzed using the daily as-run temperatures for every compact. The predicted irradiation temperatures (Hawkes 2021) were applied at the outer surface of the OPyC layer. The release from the fuel particles includes a uranium contamination fraction of 4.95×10^{-6} for capsules 1 and 5 and 5.02×10^{-6} for capsules 2 through 4. Compact release fraction results for silver (Figure 10), cesium (Figure 11), and strontium (Figure 12) are illustrated below with the tabulated results presented in Appendix B. The results are based on the number of atoms released from 2265 (capsules 2, 3, and 4) and 3393 (capsules 1 and 5) fuel particles.

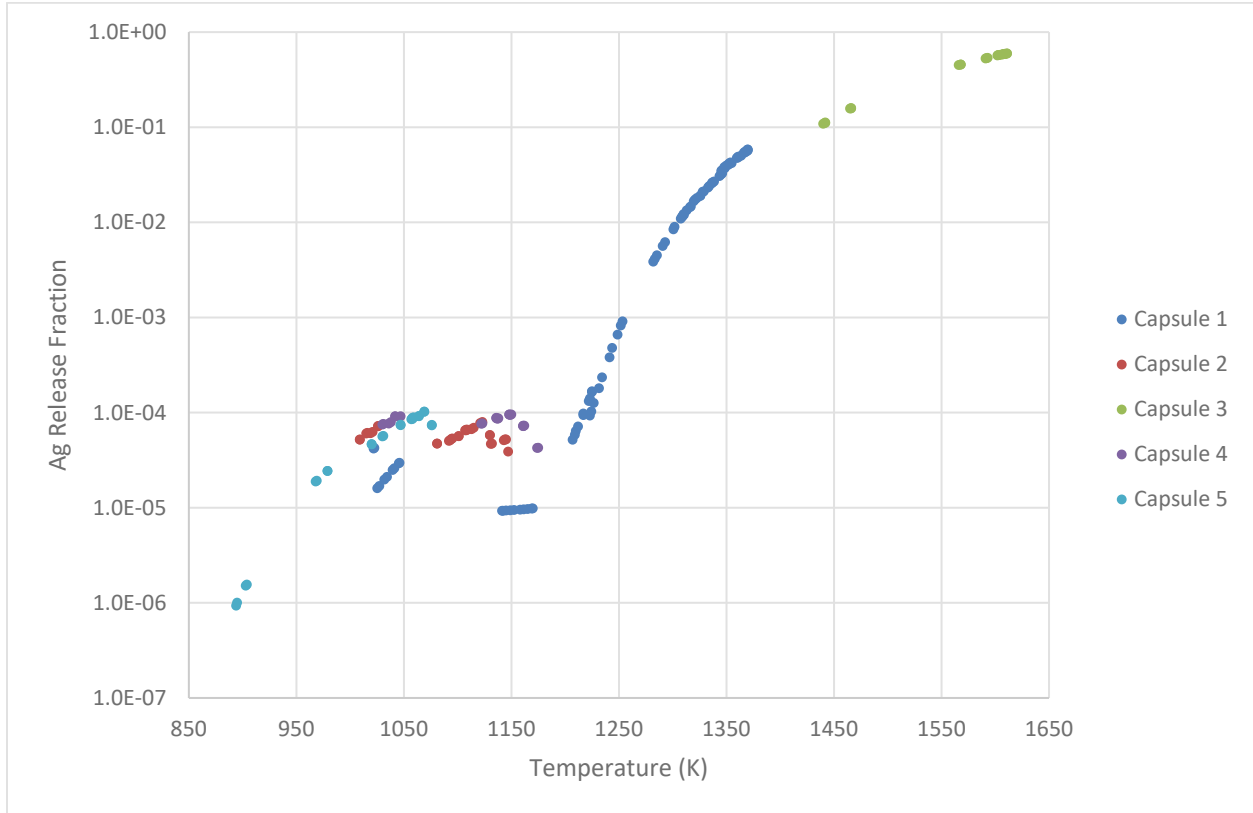


Figure 10. Compact silver (Ag) release fraction versus temperature.

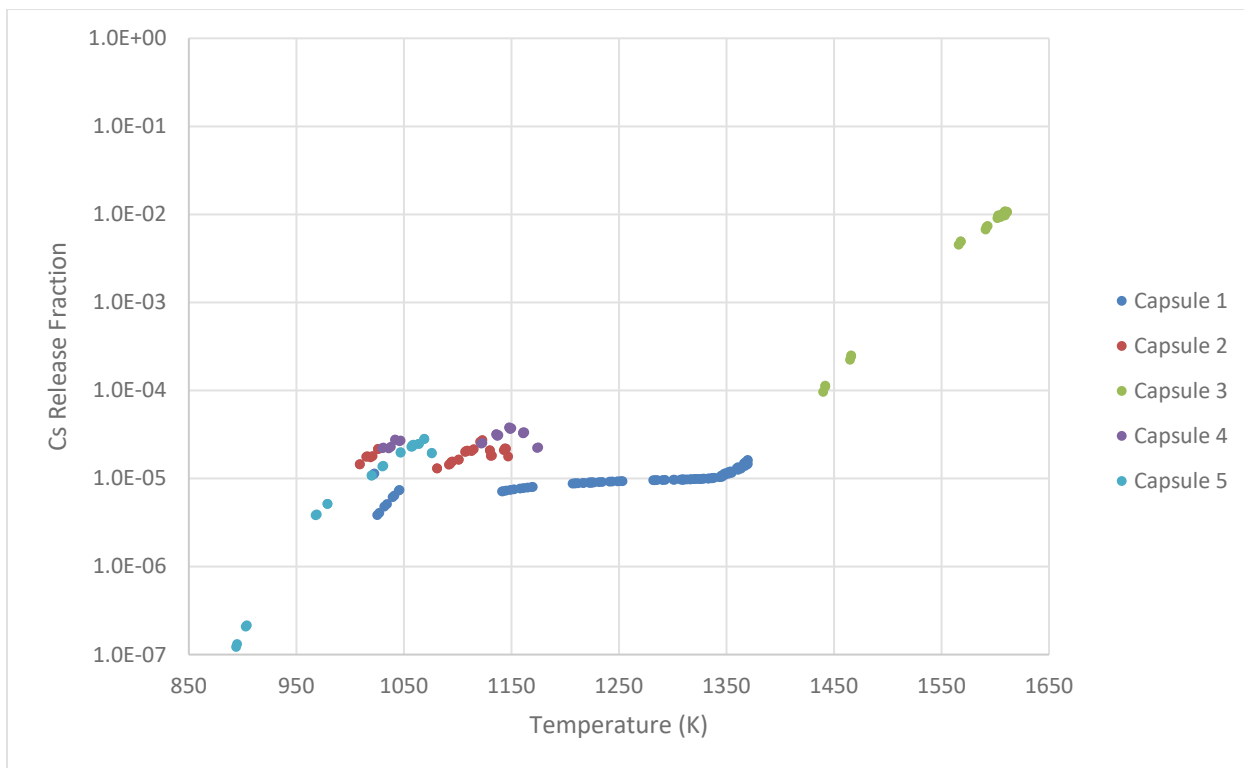


Figure 11. Compact cesium (Cs) release fraction versus temperature.

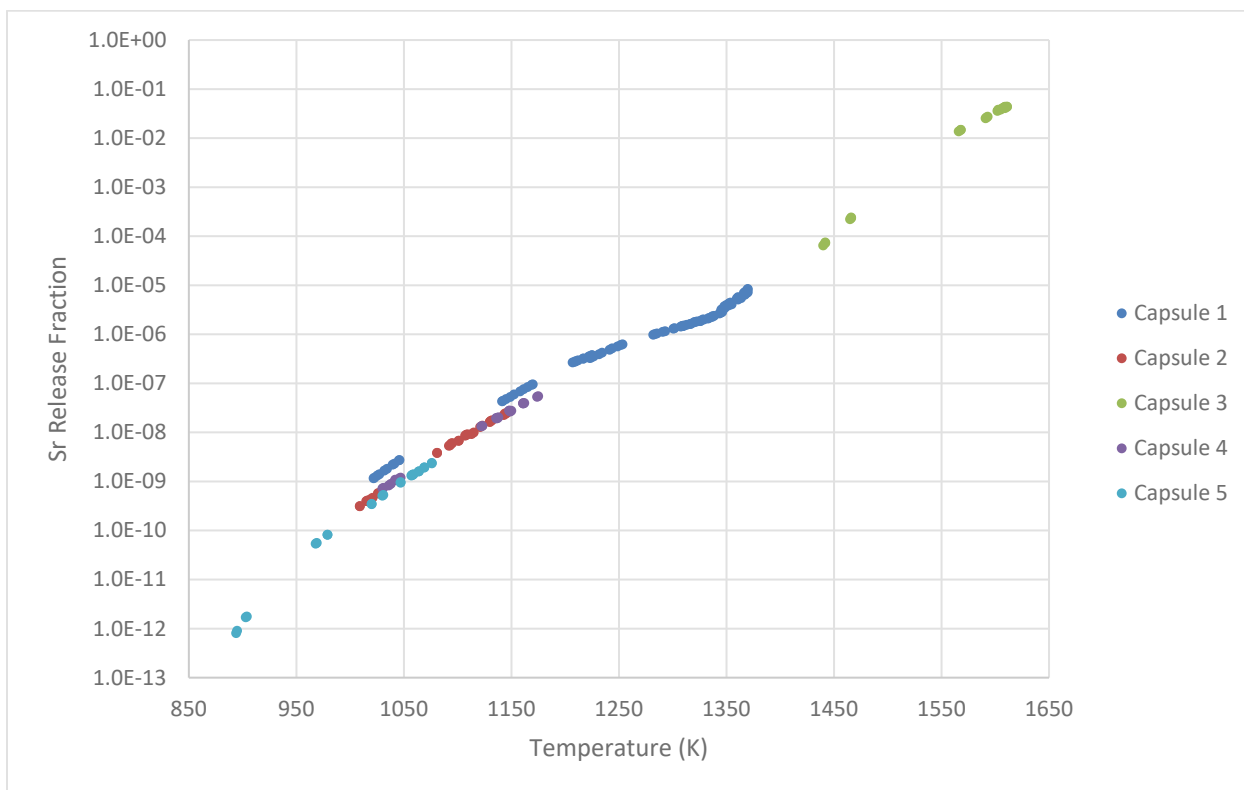


Figure 12. Compact strontium (Sr) release fraction versus temperature.

5. CONCLUSION

Fuel particle failure analysis was completed using PARFUME to analyze the failure probability of the AGR-5/6/7 irradiation test using the as-run physics and thermal analyses. The AGR-5/6/7 test was an irradiation of five capsules in the NEFT position of ATR for approximately 376 EFPDs. Using predicted neutronic physics and thermal data, the fuel particle failure probability, buffer-IPyC gap formation, and fission product release from the TRISO fuel particles have been analyzed. The following summarizes the results derived from this work.

Failure probabilities are predicted to be low, resulting in fuel particle failures in compacts only in capsule 2 and capsule 5.

The irradiation conditions of the AGR-5/6/7 test result in a prediction of zero fuel particle failures in the compacts in capsules 1, 3, and 4. Fuel particle failures were predicted in two of the compacts in capsule 2 (compacts 2-1-1 and 2-1-2). One particle failure is predicted in each one of the compacts in capsule 5. All compacts that exhibited fuel particle failures predicted by PARFUME were caused by localized stress concentrations in the SiC layer caused by cracking in the IPyC layer. These compacts experienced lower irradiation temperatures resulting in a slower creep rate of the pyrocarbon layers which caused an increase in localized stresses and consequently, an increase in the probability of IPyC cracking.

Irradiation-induced shrinkage of the buffer and IPyC layer resulted in the formation of a buffer-IPyC gap.

As expected, shrinkage of the buffer and IPyC layer during irradiation resulted in formation of a buffer-IPyC gap. Compacts with a lower irradiation temperature and fluence experienced the smallest buffer-IPyC gap formation. Conversely, higher irradiated temperature compacts with a high fluence experienced the largest buffer-IPyC gap formation. Compact 3-6-3 experienced the largest buffer-IPyC gap formation of just under 21.7 μm .

The release fraction of fission products varies depending on temperature.

The release fraction of fission products Ag, Cs, and Sr vary depending on capsule location and irradiation temperature. The maximum release fraction of Ag occurs in capsule 3, reaching up to 59.5% for the TRISO fuel particles (compact 3-6-3). The release fraction of the other two fission products, Cs and Sr, are much smaller. A maximum Cs release fraction of 1.1% occurred in compact 3-4-3 and 4.4% for Sr in compact 3-6-3.

6. REFERENCES

- Abaqus, 2009, *Abaqus User's Manual*, Dassault Systemes Simulia Corp.
- ASME, "Quality Assurance Requirements for Nuclear Facility Applications," NQA-1-2008/-1a-2009, American Society of Mechanical Engineers, March 2008 (Addenda August 2009).
- CEGA, "NP-MHTGR Material Models of Pyrocarbon and Pyrolytic Silicon Carbide," CEGA-002820, Rev. 1, CEGA Corporation, San Diego, CA, July 1993.
- Collin, B. P., "AGR-5/6/7 Irradiation Experiment Test Plan," PLN-5245, Rev. 1, Idaho National Laboratory, January 25, 2018.
- Demkowicz, P. A., "Technical Program Plan for INL Advanced Reactor Technologies Advanced Gas Reactor Fuel Development and Qualification Program," PLN-3636, Rev. 10, Idaho National Laboratory, June 22, 2021.
- Hawkes, G. L., "AGR-5/6/7 Daily As-Run Thermal Analysis," ECAR-5633, Rev. 0, Idaho National Laboratory, August 2021.

- Marshall, D. W., “AGR-5/6/7 Fuel Specification,” SPC-1352, Rev. 8, Idaho National Laboratory, March 9, 2017.
- Maki, J. T., “AGR-5/6/7 Irradiation Test Specification,” SPC-1749, Rev. 0, Idaho National Laboratory, July 8, 2015.
- Miller, G. K., D. A. Petti, D. J. Varacalle Jr., and J. T. Maki, “Statistical approach and benchmarking for modeling of multi-dimensional behavior in TRISO-coated fuel particles,” *Journal of Nuclear Materials*, Volume 317, April 2003, pp. 69–82.
- Miller, G. K., D. A. Petti, and J. T. Maki, “Consideration of the effects of partial debonding of the IPyC and particle asphericity on TRISO-coated fuel behavior,” *Journal of Nuclear Materials*, Volume 334, September 2004, pp. 79–89.
- Miller, G. K., and D. L. Knudson, “Advanced Gas Reactor-1 Pre-Test Prediction Analyses Using the PARFUME Code,” EDF-5741, Rev. 1, Idaho National Laboratory, April 25, 2007.
- Miller, G. K., D. A. Petti, J. T. Maki, D. L. Knudson, W. F. Skerjanc, “PARFUME Theory and Model Basis Report,” INL/EXT-08-14497, Rev. 1, Idaho National Laboratory, September 2018.
- Pham, B. T., J. Palmer, D. W. Marshall, G. L. Hawkes, D. M. Scates, and P. A. Demkowicz, “AGR-5/6/7 Irradiation Test Final As-Run Report,” INL/EXT-21-64221, Rev. 0, Idaho National Laboratory, September 2021.
- Skerjanc, W. F., J. T. Maki, B. P. Collin, and D. A. Petti “Evaluation of design parameters for TRISO-coated fuel particles to establish manufacturing critical limits using PARFUME,” *Journal of Nuclear Materials*, Volume 469, February 2016, pp. 99–105.
- Skerjanc, W. F., “AGR-5/6/7 Irradiation Test Predictions using PARFUME,” INL/EXT-17-43189, Rev. 0, Idaho National Laboratory, September 2017.
- Sterbentz, J. W., “JMOCUP Physics Depletion Calculations for the As-Run AGR-5/6/7 TRISO Particle Experiment in ATR Northeast Flux Trap,” ECAR-5321, Rev. 0, Idaho National Laboratory, December 2020.

Appendix A

Fuel Particle Failure Probability

Table A1. AGR-5/6/7 capsule 5 fuel particle failure probability.

Compact	Fluence (× 10 ²⁵ n/m ²) [E _n > 0.18 MeV]	Burnup (% FIMA)	Temperature (°C)	Probability of				Estimated Number of Particle Failures
				SiC Failure	Failure due to		IPyC Cracking	
					IPyC Cracking	Pressure		
5-6-4	1.74	7.05	631	4.21E-04	4.21E-04	0.00E+00	8.64E-01	1
5-6-3	1.74	7.03	630	4.21E-04	4.21E-04	0.00E+00	8.64E-01	1
5-6-2	1.67	6.75	621	4.34E-04	4.34E-04	0.00E+00	8.64E-01	1
5-6-1	1.68	6.75	622	4.32E-04	4.32E-04	0.00E+00	8.64E-01	1
5-5-4	2.14	7.67	758	2.34E-04	2.34E-04	0.00E+00	8.24E-01	1
5-5-3	2.13	7.64	757	2.35E-04	2.35E-04	0.00E+00	8.24E-01	1
5-5-2	2.05	7.44	747	2.52E-04	2.52E-04	0.00E+00	8.29E-01	1
5-5-1	2.06	7.43	747	2.51E-04	2.51E-04	0.00E+00	8.29E-01	1
5-4-4	2.49	8.17	803	1.71E-04	1.71E-04	0.00E+00	7.92E-01	1
5-4-3	2.48	8.16	803	1.72E-04	1.72E-04	0.00E+00	7.92E-01	1
5-4-2	2.39	7.96	791	1.86E-04	1.86E-04	0.00E+00	7.99E-01	1
5-4-1	2.40	7.98	791	1.86E-04	1.86E-04	0.00E+00	8.00E-01	1
5-3-4	2.82	8.60	796	1.85E-04	1.85E-04	0.00E+00	8.19E-01	1
5-3-3	2.81	8.59	796	1.84E-04	1.84E-04	0.00E+00	8.18E-01	1
5-3-2	2.70	8.43	784	1.97E-04	1.97E-04	0.00E+00	8.22E-01	1
5-3-1	2.71	8.43	785	1.96E-04	1.96E-04	0.00E+00	8.21E-01	1
5-2-4	3.13	8.99	785	2.02E-04	2.02E-04	0.00E+00	8.39E-01	1
5-2-3	3.12	8.98	786	2.01E-04	2.01E-04	0.00E+00	8.38E-01	1
5-2-2	2.99	8.82	774	2.13E-04	2.13E-04	0.00E+00	8.40E-01	1
5-2-1	3.01	8.84	774	2.12E-04	2.12E-04	0.00E+00	8.40E-01	1
5-1-4	3.40	9.40	706	3.12E-04	3.12E-04	0.00E+00	8.66E-01	1
5-1-3	3.39	9.38	706	3.12E-04	3.12E-04	0.00E+00	8.66E-01	1
5-1-2	3.25	9.17	695	3.24E-04	3.24E-04	0.00E+00	8.66E-01	1
5-1-1	3.27	9.16	696	3.22E-04	3.22E-04	0.00E+00	8.66E-01	1

Table A2. AGR-5/6/7 capsule 4 fuel particle failure probability.

Compact	Fluence (× 10 ²⁵ n/m ²) [E _n > 0.18 MeV]	Burnup (% FIMA)	Temperature (°C)	Probability of				Estimated Number of Particle Failures
				SiC Failure	Failure due to		IPyC Cracking	
					IPyC Cracking	Pressure		
4-6-4	4.20	12.65	774	1.94E-04	1.94E-04	0.00E+00	8.38E-01	0
4-6-3	4.18	12.62	773	1.95E-04	1.95E-04	0.00E+00	8.38E-01	0
4-6-2	4.00	12.35	763	2.06E-04	2.06E-04	0.00E+00	8.40E-01	0
4-6-1	4.01	12.37	765	2.02E-04	2.02E-04	0.00E+00	8.39E-01	0
4-5-4	4.44	13.15	877	7.29E-05	7.29E-05	0.00E+00	6.62E-01	0
4-5-3	4.42	13.11	876	7.39E-05	7.39E-05	0.00E+00	6.64E-01	0
4-5-2	4.23	12.83	864	8.09E-05	8.09E-05	0.00E+00	6.73E-01	0
4-5-1	4.24	12.84	865	7.93E-05	7.93E-05	0.00E+00	6.69E-01	0
4-4-4	4.62	13.56	902	5.15E-05	5.15E-05	0.00E+00	5.84E-01	0
4-4-3	4.61	13.52	901	5.22E-05	5.22E-05	0.00E+00	5.87E-01	0
4-4-2	4.40	13.21	888	5.83E-05	5.83E-05	0.00E+00	6.01E-01	0
4-4-1	4.42	13.24	888	5.78E-05	5.78E-05	0.00E+00	5.99E-01	0
4-3-4	4.79	13.87	888	6.03E-05	6.03E-05	0.00E+00	6.20E-01	0
4-3-3	4.77	13.83	889	6.01E-05	6.01E-05	0.00E+00	6.20E-01	0
4-3-2	4.55	13.53	875	6.81E-05	6.81E-05	0.00E+00	6.37E-01	0
4-3-1	4.57	13.55	875	6.74E-05	6.74E-05	0.00E+00	6.35E-01	0
4-2-4	4.93	14.07	863	8.39E-05	8.39E-05	0.00E+00	7.00E-01	0
4-2-3	4.90	14.02	863	8.33E-05	8.33E-05	0.00E+00	6.98E-01	0
4-2-2	4.68	13.70	849	9.35E-05	9.35E-05	0.00E+00	7.13E-01	0
4-2-1	4.70	13.72	850	9.27E-05	9.27E-05	0.00E+00	7.11E-01	0
4-1-4	5.03	14.09	769	1.96E-04	1.96E-04	0.00E+00	8.46E-01	0
4-1-3	5.01	14.06	769	1.95E-04	1.95E-04	0.00E+00	8.45E-01	0
4-1-2	4.78	13.72	757	2.09E-04	2.09E-04	0.00E+00	8.49E-01	0
4-1-1	4.80	13.77	758	2.08E-04	2.08E-04	0.00E+00	8.48E-01	0

Table A3. AGR-5/6/7 capsule 3 fuel particle failure probability.

Compact	Fluence (× 10 ²⁵ n/m ²) [E _n > 0.18 MeV]	Burnup (% FIMA)	Temperature (°C)	Probability of				Estimated Number of Particle Failures
				SiC Failure	Failure due to		IPyC Cracking	
					IPyC Cracking	Pressure		
3-8-3	5.30	13.81	1193	1.07E-07	1.07E-07	0.00E+00	2.32E-02	0
3-8-2	5.29	13.80	1193	1.07E-07	1.07E-07	0.00E+00	2.35E-02	0
3-8-1	5.18	13.62	1192	1.11E-07	1.11E-07	0.00E+00	2.37E-02	0
3-7-3	5.41	14.49	1320	5.22E-09	5.22E-09	3.50E-12	4.43E-03	0
3-7-2	5.40	14.46	1319	5.35E-09	5.35E-09	2.52E-12	4.48E-03	0
3-7-1	5.28	14.27	1318	5.11E-09	5.11E-09	8.50E-13	4.26E-03	0
3-6-3	5.47	14.77	1338	3.54E-09	3.40E-09	1.44E-10	3.53E-03	0
3-6-2	5.46	14.72	1338	3.53E-09	3.41E-09	1.16E-10	3.53E-03	0
3-6-1	5.34	14.56	1336	3.39E-09	3.34E-09	5.16E-11	3.40E-03	0
3-5-3	5.52	14.89	1334	3.73E-09	3.60E-09	1.32E-10	3.63E-03	0
3-5-2	5.51	14.86	1334	3.75E-09	3.62E-09	1.22E-10	3.65E-03	0
3-5-1	5.39	14.69	1332	3.58E-09	3.52E-09	5.19E-11	3.49E-03	0
3-4-3	5.54	14.95	1336	3.51E-09	3.29E-09	2.17E-10	3.44E-03	0
3-4-2	5.54	14.91	1336	3.51E-09	3.32E-09	1.91E-10	3.46E-03	0
3-4-1	5.41	14.73	1335	3.27E-09	3.17E-09	9.25E-11	3.28E-03	0
3-3-3	5.55	14.88	1330	3.94E-09	3.85E-09	8.74E-11	3.77E-03	0
3-3-2	5.55	14.84	1330	3.93E-09	3.86E-09	7.59E-11	3.77E-03	0
3-3-1	5.42	14.67	1329	3.75E-09	3.72E-09	3.52E-11	3.60E-03	0
3-2-3	5.54	14.62	1295	8.85E-09	8.85E-09	6.45E-14	5.92E-03	0
3-2-2	5.54	14.61	1295	8.83E-09	8.83E-09	5.74E-14	5.89E-03	0
3-2-1	5.42	14.43	1293	8.58E-09	8.58E-09	1.27E-14	5.66E-03	0
3-1-3	5.49	13.77	1169	2.12E-07	2.12E-07	0.00E+00	3.52E-02	0
3-1-2	5.48	13.76	1169	2.17E-07	2.17E-07	0.00E+00	3.56E-02	0
3-1-1	5.37	13.58	1167	2.22E-07	2.22E-07	0.00E+00	3.63E-02	0

Table A4. AGR-5/6/7 capsule 2 fuel particle failure probability.

Compact	Fluence ($\times 10^{25}$ n/m ²) [E _n > 0.18 MeV]	Burnup (% FIMA)	Temperature (°C)	Probability of				Estimated Number of Particle Failures
				SiC Failure	Failure due to		IPyC Cracking	
					IPyC Cracking	Pressure		
2-8-4	5.44	15.26	753	2.04E-04	2.04E-04	0.00E+00	8.35E-01	0
2-8-3	5.44	15.25	753	2.03E-04	2.03E-04	0.00E+00	8.35E-01	0
2-8-2	5.20	14.93	742	2.17E-04	2.17E-04	0.00E+00	8.40E-01	0
2-8-1	5.21	14.93	743	2.15E-04	2.15E-04	0.00E+00	8.38E-01	0
2-7-4	5.42	15.26	819	1.07E-04	1.07E-04	0.00E+00	7.06E-01	0
2-7-3	5.42	15.25	820	1.06E-04	1.06E-04	0.00E+00	7.04E-01	0
2-7-2	5.17	14.92	808	1.17E-04	1.17E-04	0.00E+00	7.19E-01	0
2-7-1	5.18	14.92	808	1.17E-04	1.17E-04	0.00E+00	7.18E-01	0
2-6-4	5.36	15.21	834	8.62E-05	8.62E-05	0.00E+00	6.45E-01	0
2-6-3	5.36	15.21	835	8.52E-05	8.52E-05	0.00E+00	6.43E-01	0
2-6-2	5.12	14.88	822	9.60E-05	9.60E-05	0.00E+00	6.64E-01	0
2-6-1	5.13	14.89	821	9.65E-05	9.65E-05	0.00E+00	6.65E-01	0
2-5-4	5.29	15.09	848	7.08E-05	7.08E-05	0.00E+00	5.93E-01	0
2-5-3	5.28	15.09	850	6.87E-05	6.87E-05	0.00E+00	5.87E-01	0
2-5-2	5.04	14.78	836	7.96E-05	7.96E-05	0.00E+00	6.14E-01	0
2-5-1	5.05	14.78	835	8.03E-05	8.03E-05	0.00E+00	6.16E-01	0
2-4-4	5.19	14.92	871	5.19E-05	5.19E-05	0.00E+00	5.21E-01	0
2-4-3	5.18	14.91	874	5.00E-05	5.00E-05	0.00E+00	5.13E-01	0
2-4-2	4.95	14.61	859	5.87E-05	5.87E-05	0.00E+00	5.41E-01	0
2-4-1	4.96	14.60	858	5.90E-05	5.90E-05	0.00E+00	5.42E-01	0
2-3-4	5.07	14.69	870	5.51E-05	5.51E-05	0.00E+00	5.37E-01	0
2-3-3	5.07	14.67	872	5.31E-05	5.31E-05	0.00E+00	5.29E-01	0
2-3-2	4.85	14.36	857	6.17E-05	6.17E-05	0.00E+00	5.55E-01	0
2-3-1	4.85	14.38	857	6.18E-05	6.18E-05	0.00E+00	5.55E-01	0
2-2-4	4.94	14.33	840	8.70E-05	8.70E-05	0.00E+00	6.51E-01	0
2-2-3	4.94	14.33	842	8.43E-05	8.43E-05	0.00E+00	6.43E-01	0
2-2-2	4.72	14.02	828	9.47E-05	9.47E-05	0.00E+00	6.63E-01	0
2-2-1	4.72	14.03	828	9.49E-05	9.49E-05	0.00E+00	6.63E-01	0
2-1-4	4.77	13.81	746	2.14E-04	2.14E-04	0.00E+00	8.36E-01	0
2-1-3	4.77	13.82	748	2.12E-04	2.12E-04	0.00E+00	8.34E-01	0
2-1-2	4.56	13.52	736	2.25E-04	2.25E-04	0.00E+00	8.39E-01	1
2-1-1	4.56	13.51	736	2.25E-04	2.25E-04	0.00E+00	8.39E-01	1

Table A5. AGR-5/6/7 capsule 1 fuel particle failure probability.

Compact	Fluence ($\times 10^{25}$ n/m ²) [E _n > 0.18 MeV]	Burnup (% FIMA)	Temperature (°C)	Probability of				Estimated Number of Particle Failures
				SiC Failure	Failure due to		IPyC Cracking	
					IPyC Cracking	Pressure		
1-9-10	4.22	11.24	937	5.31E-06	5.31E-06	0.00E+00	1.43E-01	0
1-9-9	4.31	11.40	944	4.88E-06	4.88E-06	0.00E+00	1.38E-01	0
1-9-8	4.38	11.57	950	4.53E-06	4.53E-06	0.00E+00	1.34E-01	0
1-9-7	4.40	11.67	952	4.35E-06	4.35E-06	0.00E+00	1.31E-01	0
1-9-6	4.40	11.68	952	4.39E-06	4.39E-06	0.00E+00	1.32E-01	0
1-9-5	4.38	11.53	949	4.68E-06	4.68E-06	0.00E+00	1.37E-01	0
1-9-4	4.31	11.33	944	4.99E-06	4.99E-06	0.00E+00	1.40E-01	0
1-9-3	4.22	11.22	939	5.19E-06	5.19E-06	0.00E+00	1.41E-01	0
1-9-2	4.16	11.12	936	5.36E-06	5.36E-06	0.00E+00	1.43E-01	0
1-9-1	4.17	11.09	934	5.54E-06	5.54E-06	0.00E+00	1.45E-01	0
1-8-10	4.06	10.49	1079	1.52E-07	1.52E-07	0.00E+00	1.88E-02	0
1-8-9	4.14	10.62	1088	1.33E-07	1.33E-07	0.00E+00	1.77E-02	0
1-8-8	4.21	10.76	1094	1.21E-07	1.21E-07	0.00E+00	1.70E-02	0
1-8-7	4.23	10.91	1097	1.16E-07	1.16E-07	0.00E+00	1.67E-02	0
1-8-6	4.23	10.89	1097	1.18E-07	1.18E-07	0.00E+00	1.68E-02	0
1-8-5	4.21	10.75	1093	1.28E-07	1.28E-07	0.00E+00	1.77E-02	0
1-8-4	4.14	10.59	1087	1.42E-07	1.42E-07	0.00E+00	1.85E-02	0
1-8-3	4.06	10.49	1081	1.52E-07	1.52E-07	0.00E+00	1.89E-02	0
1-8-2	4.00	10.44	1077	1.58E-07	1.58E-07	0.00E+00	1.92E-02	0
1-8-1	4.00	10.43	1075	1.64E-07	1.64E-07	0.00E+00	1.95E-02	0
1-7-10	3.82	10.04	1079	1.50E-07	1.50E-07	0.00E+00	1.82E-02	0
1-7-9	3.90	10.13	1088	1.30E-07	1.30E-07	0.00E+00	1.71E-02	0
1-7-8	3.97	10.22	1094	1.18E-07	1.18E-07	0.00E+00	1.64E-02	0
1-7-7	3.99	10.34	1097	1.14E-07	1.14E-07	0.00E+00	1.61E-02	0
1-7-6	3.99	10.36	1096	1.17E-07	1.17E-07	0.00E+00	1.64E-02	0
1-7-5	3.97	10.19	1091	1.33E-07	1.33E-07	0.00E+00	1.76E-02	0
1-7-4	3.90	10.12	1082	1.55E-07	1.55E-07	0.00E+00	1.89E-02	0
1-7-3	3.82	10.02	1076	1.66E-07	1.66E-07	0.00E+00	1.94E-02	0
1-7-2	3.76	10.01	1072	1.72E-07	1.72E-07	0.00E+00	1.96E-02	0
1-7-1	3.76	10.00	1073	1.68E-07	1.68E-07	0.00E+00	1.94E-02	0
1-6-10	3.55	9.64	1055	2.83E-07	2.83E-07	0.00E+00	2.57E-02	0
1-6-9	3.62	9.70	1064	2.43E-07	2.43E-07	0.00E+00	2.38E-02	0
1-6-8	3.68	9.78	1071	2.19E-07	2.19E-07	0.00E+00	2.28E-02	0
1-6-7	3.70	9.86	1073	2.08E-07	2.08E-07	0.00E+00	2.22E-02	0
1-6-6	3.70	9.88	1072	2.15E-07	2.15E-07	0.00E+00	2.26E-02	0
1-6-5	3.68	9.79	1066	2.52E-07	2.52E-07	0.00E+00	2.47E-02	0
1-6-4	3.62	9.68	1056	3.01E-07	3.01E-07	0.00E+00	2.70E-02	0
1-6-3	3.54	9.63	1050	3.28E-07	3.28E-07	0.00E+00	2.80E-02	0

Compact	Fluence ($\times 10^{25}$ n/m ²) [E _n > 0.18 MeV]	Burnup (% FIMA)	Temperature (°C)	Probability of				Estimated Number of Particle Failures
				SiC Failure	Failure due to		IPyC Cracking	
					IPyC Cracking	Pressure		
1-6-2	3.49	9.61	1047	3.37E-07	3.37E-07	0.00E+00	2.82E-02	0
1-6-1	3.49	9.61	1048	3.26E-07	3.26E-07	0.00E+00	2.76E-02	0
1-5-10	3.24	9.23	1043	3.82E-07	3.82E-07	0.00E+00	2.99E-02	0
1-5-9	3.30	9.29	1053	3.17E-07	3.17E-07	0.00E+00	2.72E-02	0
1-5-8	3.36	9.38	1060	2.73E-07	2.73E-07	0.00E+00	2.52E-02	0
1-5-7	3.39	9.46	1064	2.50E-07	2.50E-07	0.00E+00	2.40E-02	0
1-5-6	3.39	9.46	1061	2.68E-07	2.68E-07	0.00E+00	2.50E-02	0
1-5-5	3.37	9.36	1053	3.27E-07	3.27E-07	0.00E+00	2.79E-02	0
1-5-4	3.30	9.27	1044	3.94E-07	3.94E-07	0.00E+00	3.08E-02	0
1-5-3	3.23	9.21	1038	4.43E-07	4.43E-07	0.00E+00	3.25E-02	0
1-5-2	3.18	9.19	1035	4.62E-07	4.62E-07	0.00E+00	3.30E-02	0
1-5-1	3.19	9.17	1036	4.45E-07	4.45E-07	0.00E+00	3.24E-02	0
1-4-10	2.89	8.74	1018	7.01E-07	7.01E-07	0.00E+00	4.09E-02	0
1-4-9	2.96	8.82	1028	5.51E-07	5.51E-07	0.00E+00	3.60E-02	0
1-4-8	3.02	8.95	1036	4.47E-07	4.47E-07	0.00E+00	3.21E-02	0
1-4-7	3.04	9.03	1040	3.97E-07	3.97E-07	0.00E+00	3.00E-02	0
1-4-6	3.04	9.05	1037	4.26E-07	4.26E-07	0.00E+00	3.12E-02	0
1-4-5	3.02	8.95	1029	5.35E-07	5.35E-07	0.00E+00	3.55E-02	0
1-4-4	2.96	8.80	1020	6.81E-07	6.81E-07	0.00E+00	4.06E-02	0
1-4-3	2.89	8.73	1012	8.06E-07	8.06E-07	0.00E+00	4.44E-02	0
1-4-2	2.84	8.69	1009	8.70E-07	8.70E-07	0.00E+00	4.61E-02	0
1-4-1	2.85	8.68	1011	8.34E-07	8.34E-07	0.00E+00	4.49E-02	0
1-3-10	2.52	8.17	958	3.02E-06	3.02E-06	0.00E+00	9.18E-02	0
1-3-9	2.58	8.29	968	2.37E-06	2.37E-06	0.00E+00	8.03E-02	0
1-3-8	2.63	8.40	976	1.93E-06	1.93E-06	0.00E+00	7.15E-02	0
1-3-7	2.66	8.50	980	1.69E-06	1.69E-06	0.00E+00	6.65E-02	0
1-3-6	2.65	8.50	979	1.77E-06	1.77E-06	0.00E+00	6.82E-02	0
1-3-5	2.63	8.40	971	2.20E-06	2.20E-06	0.00E+00	7.72E-02	0
1-3-4	2.58	8.26	961	2.81E-06	2.81E-06	0.00E+00	8.87E-02	0
1-3-3	2.52	8.15	954	3.39E-06	3.39E-06	0.00E+00	9.81E-02	0
1-3-2	2.48	8.11	950	3.70E-06	3.70E-06	0.00E+00	1.03E-01	0
1-3-1	2.48	8.11	951	3.57E-06	3.57E-06	0.00E+00	1.01E-01	0
1-2-10	2.11	7.42	876	1.98E-05	1.98E-05	0.00E+00	2.61E-01	0
1-2-9	2.16	7.58	885	1.63E-05	1.63E-05	0.00E+00	2.35E-01	0
1-2-8	2.20	7.73	892	1.38E-05	1.38E-05	0.00E+00	2.15E-01	0
1-2-7	2.23	7.85	897	1.23E-05	1.23E-05	0.00E+00	2.02E-01	0
1-2-6	2.23	7.84	896	1.26E-05	1.26E-05	0.00E+00	2.04E-01	0
1-2-5	2.21	7.71	888	1.49E-05	1.49E-05	0.00E+00	2.24E-01	0
1-2-4	2.16	7.56	880	1.81E-05	1.81E-05	0.00E+00	2.49E-01	0

Compact	Fluence ($\times 10^{25}$ n/m ²) [E _n > 0.18 MeV]	Burnup (% FIMA)	Temperature (°C)	Probability of				Estimated Number of Particle Failures
				SiC Failure	Failure due to		IPyC Cracking	
					IPyC Cracking	Pressure		
1-2-3	2.11	7.42	872	2.13E-05	2.13E-05	0.00E+00	2.72E-01	0
1-2-2	2.07	7.35	868	2.30E-05	2.30E-05	0.00E+00	2.83E-01	0
1-2-1	2.07	7.34	869	2.26E-05	2.26E-05	0.00E+00	2.80E-01	0
1-1-10	1.65	5.89	754	1.33E-04	1.33E-04	0.00E+00	6.65E-01	0
1-1-9	1.69	6.16	761	1.21E-04	1.21E-04	0.00E+00	6.41E-01	0
1-1-8	1.73	6.42	768	1.10E-04	1.10E-04	0.00E+00	6.15E-01	0
1-1-7	1.75	6.67	773	1.03E-04	1.03E-04	0.00E+00	5.98E-01	0
1-1-6	1.75	6.63	772	1.04E-04	1.04E-04	0.00E+00	5.99E-01	0
1-1-5	1.73	6.47	767	1.12E-04	1.12E-04	0.00E+00	6.20E-01	0
1-1-4	1.69	6.13	759	1.24E-04	1.24E-04	0.00E+00	6.48E-01	0
1-1-3	1.64	5.86	752	1.35E-04	1.35E-04	0.00E+00	6.70E-01	0
1-1-2	1.62	5.66	749	1.41E-04	1.41E-04	0.00E+00	6.82E-01	0
1-1-1	1.62	5.78	750	1.40E-04	1.40E-04	0.00E+00	6.80E-01	0

Appendix B

Fission Product Release

Table B1. AGR-5/6/7 capsule 5 fission product release fraction.

Compact	Fluence ($\times 10^{25}$ n/m ²) [E _n > 0.18 MeV]	Burnup (% FIMA)	Temperature (°C)	Release Fraction		
				Ag	Cs	Sr
5-6-4	1.74	7.05	631	1.56E-06	2.15E-07	1.76E-12
5-6-3	1.74	7.03	630	1.51E-06	2.08E-07	1.69E-12
5-6-2	1.67	6.75	621	9.33E-07	1.22E-07	8.05E-13
5-6-1	1.68	6.75	622	1.00E-06	1.32E-07	9.03E-13
5-5-4	2.14	7.67	758	5.69E-05	1.39E-05	5.28E-10
5-5-3	2.13	7.64	757	5.60E-05	1.37E-05	5.12E-10
5-5-2	2.05	7.44	747	4.62E-05	1.08E-05	3.42E-10
5-5-1	2.06	7.43	747	4.66E-05	1.09E-05	3.49E-10
5-4-4	2.49	8.17	803	7.41E-05	1.95E-05	2.38E-09
5-4-3	2.48	8.16	803	7.32E-05	1.93E-05	2.33E-09
5-4-2	2.39	7.96	791	9.16E-05	2.47E-05	1.60E-09
5-4-1	2.40	7.98	791	9.16E-05	2.47E-05	1.60E-09
5-3-4	2.82	8.60	796	1.02E-04	2.80E-05	1.91E-09
5-3-3	2.81	8.59	796	1.02E-04	2.82E-05	1.93E-09
5-3-2	2.70	8.43	784	8.49E-05	2.29E-05	1.32E-09
5-3-1	2.71	8.43	785	8.57E-05	2.31E-05	1.34E-09
5-2-4	3.13	8.99	785	8.79E-05	2.39E-05	1.36E-09
5-2-3	3.12	8.98	786	8.89E-05	2.42E-05	1.39E-09
5-2-2	2.99	8.82	774	7.36E-05	1.96E-05	9.40E-10
5-2-1	3.01	8.84	774	7.46E-05	1.99E-05	9.66E-10
5-1-4	3.40	9.40	706	2.43E-05	5.15E-06	8.15E-11
5-1-3	3.39	9.38	706	2.43E-05	5.15E-06	8.18E-11
5-1-2	3.25	9.17	695	1.88E-05	3.81E-06	5.37E-11
5-1-1	3.27	9.16	696	1.92E-05	3.91E-06	5.55E-11

Table B2. AGR-5/6/7 capsule 4 fission product release fraction.

Compact	Fluence ($\times 10^{25}$ n/m ²) [E _n > 0.18 MeV]	Burnup (% FIMA)	Temperature (°C)	Release Fraction		
				Ag	Cs	Sr
4-6-4	4.20	12.65	774	9.15E-05	2.70E-05	1.19E-09
4-6-3	4.18	12.62	773	9.01E-05	2.65E-05	1.16E-09
4-6-2	4.00	12.35	763	7.65E-05	2.20E-05	8.25E-10
4-6-1	4.01	12.37	765	7.93E-05	2.29E-05	8.92E-10
4-5-4	4.44	13.15	877	9.53E-05	3.72E-05	2.75E-08
4-5-3	4.42	13.11	876	9.44E-05	3.64E-05	2.65E-08
4-5-2	4.23	12.83	864	8.58E-05	3.04E-05	1.94E-08
4-5-1	4.24	12.84	865	8.69E-05	3.11E-05	2.02E-08
4-4-4	4.62	13.56	902	4.26E-05	2.25E-05	5.46E-08
4-4-3	4.61	13.52	901	4.24E-05	2.23E-05	5.31E-08
4-4-2	4.40	13.21	888	7.18E-05	3.25E-05	3.86E-08
4-4-1	4.42	13.24	888	7.21E-05	3.28E-05	3.91E-08
4-3-4	4.79	13.87	888	7.27E-05	3.33E-05	3.92E-08
4-3-3	4.77	13.83	889	7.28E-05	3.34E-05	3.95E-08
4-3-2	4.55	13.53	875	9.52E-05	3.77E-05	2.75E-08
4-3-1	4.57	13.55	875	9.55E-05	3.80E-05	2.79E-08
4-2-4	4.93	14.07	863	8.74E-05	3.15E-05	1.93E-08
4-2-3	4.90	14.02	863	8.78E-05	3.18E-05	1.97E-08
4-2-2	4.68	13.70	849	7.63E-05	2.49E-05	1.33E-08
4-2-1	4.70	13.72	850	7.69E-05	2.53E-05	1.35E-08
4-1-4	5.03	14.09	769	9.05E-05	2.74E-05	1.06E-09
4-1-3	5.01	14.06	769	9.12E-05	2.76E-05	1.08E-09
4-1-2	4.78	13.72	757	7.49E-05	2.20E-05	7.17E-10
4-1-1	4.80	13.77	758	7.60E-05	2.24E-05	7.38E-10

Table B3. AGR-5/6/7 capsule 3 fission product release fraction.

Compact	Fluence ($\times 10^{25}$ n/m ²) [E _n > 0.18 MeV]	Burnup (% FIMA)	Temperature (°C)	Release Fraction		
				Ag	Cs	Sr
3-8-3	5.30	13.81	1193	1.59E-01	2.50E-04	2.40E-04
3-8-2	5.29	13.80	1193	1.58E-01	2.44E-04	2.34E-04
3-8-1	5.18	13.62	1192	1.57E-01	2.23E-04	2.21E-04
3-7-3	5.41	14.49	1320	5.34E-01	7.39E-03	2.73E-02
3-7-2	5.40	14.46	1319	5.30E-01	7.20E-03	2.64E-02
3-7-1	5.28	14.27	1318	5.27E-01	6.74E-03	2.53E-02
3-6-3	5.47	14.77	1338	5.95E-01	1.07E-02	4.38E-02
3-6-2	5.46	14.72	1338	5.94E-01	1.06E-02	4.32E-02
3-6-1	5.34	14.56	1336	5.87E-01	9.74E-03	4.06E-02
3-5-3	5.52	14.89	1334	5.82E-01	1.02E-02	4.06E-02
3-5-2	5.51	14.86	1334	5.83E-01	1.02E-02	4.06E-02
3-5-1	5.39	14.69	1332	5.75E-01	9.32E-03	3.79E-02
3-4-3	5.54	14.95	1336	5.91E-01	1.08E-02	4.36E-02
3-4-2	5.54	14.91	1336	5.90E-01	1.08E-02	4.33E-02
3-4-1	5.41	14.73	1335	5.86E-01	1.00E-02	4.13E-02
3-3-3	5.55	14.88	1330	5.71E-01	9.74E-03	3.78E-02
3-3-2	5.55	14.84	1330	5.71E-01	9.69E-03	3.76E-02
3-3-1	5.42	14.67	1329	5.67E-01	9.04E-03	3.59E-02
3-2-3	5.54	14.62	1295	4.55E-01	4.95E-03	1.47E-02
3-2-2	5.54	14.61	1295	4.54E-01	4.90E-03	1.46E-02
3-2-1	5.42	14.43	1293	4.50E-01	4.52E-03	1.37E-02
3-1-3	5.49	13.77	1169	1.12E-01	1.13E-04	7.44E-05
3-1-2	5.48	13.76	1169	1.11E-01	1.10E-04	7.21E-05
3-1-1	5.37	13.58	1167	1.08E-01	9.62E-05	6.48E-05

Table B4. AGR-5/6/7 capsule 2 fission product release fraction.

Compact	Fluence ($\times 10^{25}$ n/m ²) [E _n > 0.18 MeV]	Burnup (% FIMA)	Temperature (°C)	Release Fraction		
				Ag	Cs	Sr
2-8-4	5.44	15.26	753	7.16E-05	2.15E-05	5.67E-10
2-8-3	5.44	15.25	753	7.22E-05	2.17E-05	5.78E-10
2-8-2	5.20	14.93	742	6.02E-05	1.76E-05	3.94E-10
2-8-1	5.21	14.93	743	6.11E-05	1.79E-05	4.08E-10
2-7-4	5.42	15.26	819	5.04E-05	1.44E-05	5.33E-09
2-7-3	5.42	15.25	820	5.11E-05	1.46E-05	5.46E-09
2-7-2	5.17	14.92	808	4.71E-05	1.30E-05	3.80E-09
2-7-1	5.18	14.92	808	4.71E-05	1.30E-05	3.81E-09
2-6-4	5.36	15.21	834	6.49E-05	2.00E-05	8.53E-09
2-6-3	5.36	15.21	835	6.60E-05	2.05E-05	8.84E-09
2-6-2	5.12	14.88	822	5.33E-05	1.56E-05	6.05E-09
2-6-1	5.13	14.89	821	5.26E-05	1.53E-05	5.91E-09
2-5-4	5.29	15.09	848	7.74E-05	2.61E-05	1.28E-08
2-5-3	5.28	15.09	850	7.94E-05	2.73E-05	1.37E-08
2-5-2	5.04	14.78	836	6.60E-05	2.07E-05	9.12E-09
2-5-1	5.05	14.78	835	6.51E-05	2.03E-05	8.85E-09
2-4-4	5.19	14.92	871	5.22E-05	2.20E-05	2.42E-08
2-4-3	5.18	14.91	874	3.89E-05	1.78E-05	2.61E-08
2-4-2	4.95	14.61	859	4.70E-05	1.82E-05	1.75E-08
2-4-1	4.96	14.60	858	4.68E-05	1.80E-05	1.72E-08
2-3-4	5.07	14.69	870	5.11E-05	2.09E-05	2.25E-08
2-3-3	5.07	14.67	872	5.20E-05	2.17E-05	2.41E-08
2-3-2	4.85	14.36	857	5.79E-05	2.09E-05	1.64E-08
2-3-1	4.85	14.38	857	5.78E-05	2.08E-05	1.63E-08
2-2-4	4.94	14.33	840	6.69E-05	2.04E-05	9.18E-09
2-2-3	4.94	14.33	842	6.91E-05	2.15E-05	9.89E-09
2-2-2	4.72	14.02	828	5.65E-05	1.64E-05	6.76E-09
2-2-1	4.72	14.03	828	5.63E-05	1.63E-05	6.72E-09
2-1-4	4.77	13.81	746	6.07E-05	1.74E-05	4.32E-10
2-1-3	4.77	13.82	748	6.26E-05	1.80E-05	4.62E-10
2-1-2	4.56	13.52	736	5.20E-05	1.45E-05	3.14E-10
2-1-1	4.56	13.51	736	5.19E-05	1.45E-05	3.12E-10

Table B5. AGR-5/6/7 capsule 1 fission product release fraction.

Compact	Fluence ($\times 10^{25}$ n/m ²) [E _n > 0.18 MeV]	Burnup (% FIMA)	Temperature (°C)	Release Fraction		
				Ag	Cs	Sr
1-9-10	4.22	11.24	937	6.41E-05	8.81E-06	2.84E-07
1-9-9	4.31	11.40	944	9.75E-05	8.91E-06	3.21E-07
1-9-8	4.38	11.57	950	1.40E-04	8.98E-06	3.56E-07
1-9-7	4.40	11.67	952	1.67E-04	9.01E-06	3.74E-07
1-9-6	4.40	11.68	952	1.64E-04	9.01E-06	3.73E-07
1-9-5	4.38	11.53	949	1.32E-04	8.97E-06	3.50E-07
1-9-4	4.31	11.33	944	9.39E-05	8.90E-06	3.18E-07
1-9-3	4.22	11.22	939	7.12E-05	8.83E-06	2.93E-07
1-9-2	4.16	11.12	936	5.83E-05	8.79E-06	2.75E-07
1-9-1	4.17	11.09	934	5.18E-05	8.76E-06	2.66E-07
1-8-10	4.06	10.49	1079	4.14E-02	1.19E-05	4.26E-06
1-8-9	4.14	10.62	1088	4.89E-02	1.34E-05	5.70E-06
1-8-8	4.21	10.76	1094	5.52E-02	1.52E-05	7.33E-06
1-8-7	4.23	10.91	1097	5.82E-02	1.62E-05	8.35E-06
1-8-6	4.23	10.89	1097	5.79E-02	1.61E-05	8.21E-06
1-8-5	4.21	10.75	1093	5.38E-02	1.48E-05	6.92E-06
1-8-4	4.14	10.59	1087	4.75E-02	1.31E-05	5.35E-06
1-8-3	4.06	10.49	1081	4.25E-02	1.20E-05	4.42E-06
1-8-2	4.00	10.44	1077	3.95E-02	1.15E-05	3.94E-06
1-8-1	4.00	10.43	1075	3.80E-02	1.13E-05	3.73E-06
1-7-10	3.82	10.04	1079	4.02E-02	1.13E-05	3.85E-06
1-7-9	3.90	10.13	1088	4.79E-02	1.25E-05	5.08E-06
1-7-8	3.97	10.22	1094	5.41E-02	1.39E-05	6.41E-06
1-7-7	3.99	10.34	1097	5.69E-02	1.46E-05	7.18E-06
1-7-6	3.99	10.36	1096	5.61E-02	1.44E-05	6.96E-06
1-7-5	3.97	10.19	1091	5.00E-02	1.30E-05	5.46E-06
1-7-4	3.90	10.12	1082	4.19E-02	1.16E-05	4.05E-06
1-7-3	3.82	10.02	1076	3.70E-02	1.10E-05	3.42E-06
1-7-2	3.76	10.01	1072	3.47E-02	1.07E-05	3.16E-06
1-7-1	3.76	10.00	1073	3.51E-02	1.08E-05	3.21E-06
1-6-10	3.55	9.64	1055	2.10E-02	9.93E-06	1.99E-06
1-6-9	3.62	9.70	1064	2.62E-02	1.01E-05	2.32E-06
1-6-8	3.68	9.78	1071	3.06E-02	1.03E-05	2.66E-06
1-6-7	3.70	9.86	1073	3.27E-02	1.05E-05	2.84E-06
1-6-6	3.70	9.88	1072	3.17E-02	1.04E-05	2.75E-06
1-6-5	3.68	9.79	1066	2.69E-02	1.02E-05	2.37E-06

Compact	Fluence ($\times 10^{25}$ n/m ²) [E _n > 0.18 MeV]	Burnup (% FIMA)	Temperature (°C)	Release Fraction		
				Ag	Cs	Sr
1-6-4	3.62	9.68	1056	2.11E-02	9.94E-06	1.99E-06
1-6-3	3.54	9.63	1050	1.80E-02	9.85E-06	1.82E-06
1-6-2	3.49	9.61	1047	1.67E-02	9.82E-06	1.74E-06
1-6-1	3.49	9.61	1048	1.73E-02	9.84E-06	1.78E-06
1-5-10	3.24	9.23	1043	1.44E-02	9.77E-06	1.62E-06
1-5-9	3.30	9.29	1053	1.89E-02	9.85E-06	1.85E-06
1-5-8	3.36	9.38	1060	2.32E-02	9.96E-06	2.09E-06
1-5-7	3.39	9.46	1064	2.57E-02	1.00E-05	2.25E-06
1-5-6	3.39	9.46	1061	2.39E-02	9.98E-06	2.14E-06
1-5-5	3.37	9.36	1053	1.90E-02	9.86E-06	1.86E-06
1-5-4	3.30	9.27	1044	1.46E-02	9.77E-06	1.63E-06
1-5-3	3.23	9.21	1038	1.20E-02	9.73E-06	1.49E-06
1-5-2	3.18	9.19	1035	1.09E-02	9.71E-06	1.43E-06
1-5-1	3.19	9.17	1036	1.15E-02	9.72E-06	1.46E-06
1-4-10	2.89	8.74	1018	5.64E-03	9.61E-06	1.12E-06
1-4-9	2.96	8.82	1028	8.43E-03	9.67E-06	1.30E-06
1-4-8	3.02	8.95	1036	1.14E-02	9.72E-06	1.46E-06
1-4-7	3.04	9.03	1040	1.34E-02	9.74E-06	1.56E-06
1-4-6	3.04	9.05	1037	1.22E-02	9.73E-06	1.50E-06
1-4-5	3.02	8.95	1029	8.95E-03	9.68E-06	1.33E-06
1-4-4	2.96	8.80	1020	6.17E-03	9.62E-06	1.15E-06
1-4-3	2.89	8.73	1012	4.50E-03	9.58E-06	1.03E-06
1-4-2	2.84	8.69	1009	3.85E-03	9.55E-06	9.80E-07
1-4-1	2.85	8.68	1011	4.12E-03	9.56E-06	1.00E-06
1-3-10	2.52	8.17	958	1.80E-04	9.07E-06	3.92E-07
1-3-9	2.58	8.29	968	3.79E-04	9.20E-06	4.82E-07
1-3-8	2.63	8.40	976	6.59E-04	9.28E-06	5.64E-07
1-3-7	2.66	8.50	980	9.08E-04	9.33E-06	6.20E-07
1-3-6	2.65	8.50	979	8.21E-04	9.31E-06	6.02E-07
1-3-5	2.63	8.40	971	4.77E-04	9.23E-06	5.14E-07
1-3-4	2.58	8.26	961	2.34E-04	9.11E-06	4.21E-07
1-3-3	2.52	8.15	954	1.26E-04	9.01E-06	3.55E-07
1-3-2	2.48	8.11	950	9.27E-05	8.96E-06	3.27E-07
1-3-1	2.48	8.11	951	1.03E-04	8.98E-06	3.36E-07
1-2-10	2.11	7.42	876	9.37E-06	7.39E-06	5.27E-08
1-2-9	2.16	7.58	885	9.51E-06	7.67E-06	6.82E-08
1-2-8	2.20	7.73	892	9.66E-06	7.88E-06	8.35E-08

Compact	Fluence ($\times 10^{25}$ n/m ²) [E _n > 0.18 MeV]	Burnup (% FIMA)	Temperature (°C)	Release Fraction		
				Ag	Cs	Sr
1-2-7	2.23	7.85	897	9.82E-06	8.00E-06	9.53E-08
1-2-6	2.23	7.84	896	9.79E-06	7.98E-06	9.31E-08
1-2-5	2.21	7.71	888	9.58E-06	7.78E-06	7.61E-08
1-2-4	2.16	7.56	880	9.43E-06	7.52E-06	5.93E-08
1-2-3	2.11	7.42	872	9.32E-06	7.27E-06	4.77E-08
1-2-2	2.07	7.35	868	9.26E-06	7.13E-06	4.28E-08
1-2-1	2.07	7.34	869	9.28E-06	7.16E-06	4.40E-08
1-1-10	1.65	5.89	754	1.69E-05	4.06E-06	1.39E-09
1-1-9	1.69	6.16	761	2.11E-05	5.13E-06	1.80E-09
1-1-8	1.73	6.42	768	2.59E-05	6.39E-06	2.30E-09
1-1-7	1.75	6.67	773	2.97E-05	7.40E-06	2.72E-09
1-1-6	1.75	6.63	772	2.93E-05	7.31E-06	2.68E-09
1-1-5	1.73	6.47	767	2.49E-05	6.13E-06	2.19E-09
1-1-4	1.69	6.13	759	1.97E-05	4.79E-06	1.66E-09
1-1-3	1.64	5.86	752	1.60E-05	3.84E-06	1.31E-09
1-1-2	1.62	5.66	749	4.18E-05	1.12E-05	1.15E-09
1-1-1	1.62	5.78	750	4.24E-05	1.14E-05	1.18E-09